

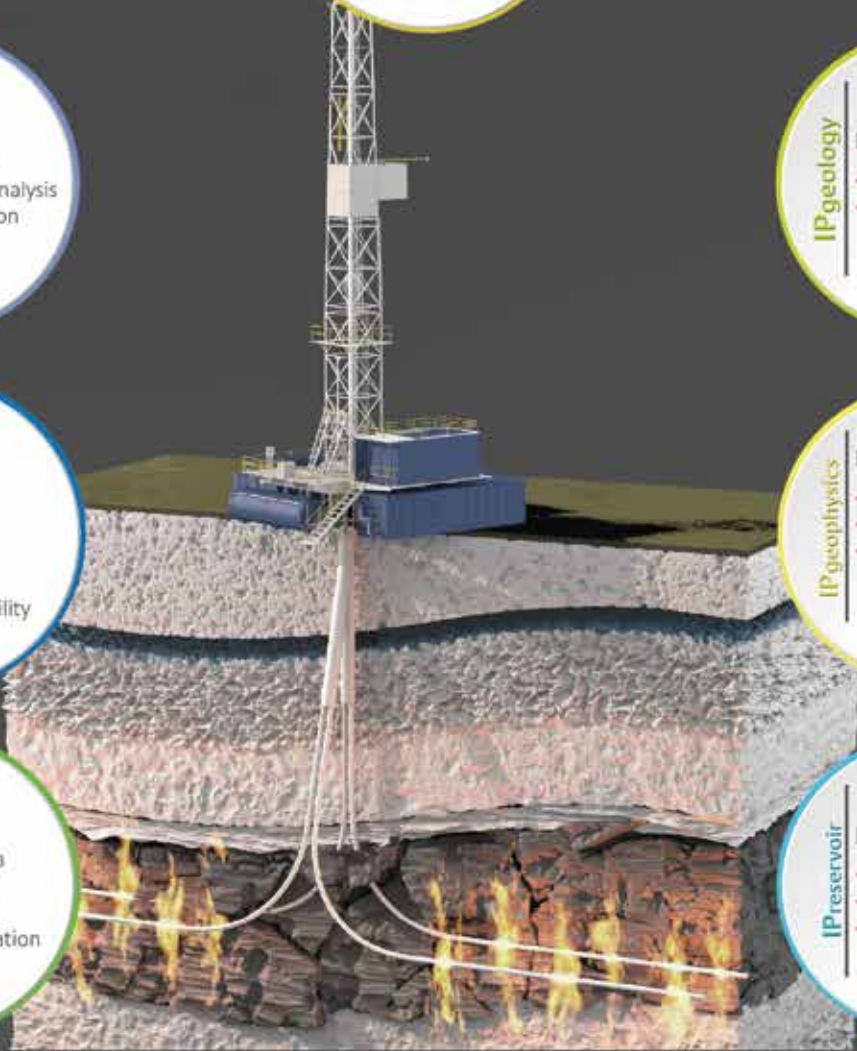


Inside...

- 4** Key Questions About Monitoring Induced Seismic Activity
- 6** Fracture Evaluation: Height & Contribution Using FMI and Advanced Diagnostic Tools
- 12** Delineation of thermally altered zones in SAGD producer wells through resistivity characterization using LWD azimuthal propagation tool
- 16** Three Methods for Log-Derived Mineralogy: Part Three ...Petrophysics Designed to Honour Core: at Work in the Montney Formation



A member of the Lloyd's Register group



IPbase

Includes...

- Deterministic Petrophysics
- Multi Well Workflows - 3D Petrophysics
- Unconventional Resources Module

IPre

Includes...

- Mineral Solver
- Monte Carlo Analysis
- Curve Prediction
- Rock Typing

IPgeology

Includes...

- Image Analysis
- Rock Typing

IPgeomechanics

Includes...

- SandPIT 3D Multi-depth
- Pore Pressure Prediction
- Well Bore Stability

IPgeophysics

Includes...

- Rock Physics
- Curve Prediction
- Acoustic Waveform Processing

IPwells

Includes...

- Chrono Log
- Real Time Data
- Pore Pressure Prediction
- Cement Evaluation
- Geosteering

IPreservoir

Includes...

- Saturation Height
- Formation Testing
- Production Logging

IP™ has the solution for your unconventional workflows

IP™ is more than just a best-in-class petrophysics package; it is also a tool for Petrophysicists, Geologists and Reservoir Engineers who want to take control of their interpretation. IP's intuitive interface enables the user to focus on their workflow allowing our industry-leading modules to offer a powerful insight into complex analyses.

Whether used for a single workflow on a single well, or as a complete solution for multi well projects, IP offers technical excellence at a competitive price.

For more information, visit www.lr-senergy.com/software/ip

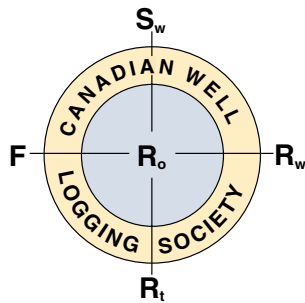
Speak to our experts

T: +1 281 846-7229 | E: Alen.Gonzalez@lr-senergy.com

InSite

CWLS Magazine

Spring 2016



Editors:
Doug Kozak and Manuel Aboud

Layout and Design:
Sherry Mumford
Connections Desktop Publishing

Advertising:
Doug Kozak and Manuel Aboud

Proof Reader:
William Neil Scott

Contributors:
Dario Baturan, Alan D. Cull,
R.V. Everett, Anand Gupta,
Sepideh Karimi, Jim Koch,
Andrew Law, Dr. Fathi Shnaib,
Ian Theunissen

Printer:
Little Rock

All material in this magazine is copyright © CWLS, unless otherwise indicated. Unauthorized use, duplication or publication prohibited without permission from the CWLS.

The InSite is an informal magazine with technical content. The material is not subject to peer review. The opinions expressed are those of the individual authors.

Table of Contents

- | | | | |
|---|--|----|---|
| 2 | CWLS 2015 to 2016 Executive | 12 | Delineation of thermally altered zones in SAGD producer wells through resistivity characterization using LWD azimuthal propagation tool |
| 3 | Presidents Report | | |
| 4 | Key Questions About Monitoring Induced Seismic Activity | 16 | Three Methods for Log-Derived Mineralogy: Part Three ... Petrophysics Designed to Honour Core: at Work in the Montney Formation |
| 6 | Fracture Evaluation: Height & Contribution Using FMI and Advanced Diagnostic Tools | | |

Cover Photo: Cardium Formation at Ram Falls, Alberta

Photo Credit: Courtesy of Per Kent Pedersen, Associate Professor, Department of Geoscience, University of Calgary

Photos: If you have photos that the CWLS can use in its next InSite please send a high resolution jpeg format version to Doug.Kozak@Halliburton.com or maboud@slb.com. Include a short description of the photo with your submission.



The 2015 to 2016 CWLS Executive:

Back row (l - r): Jamie Everett, Doug Kozak, James Ablett, Manuel Aboud, Adam Macdonald
Front row (l - r): Kathy Diaz, William Parrales, Tiffany Yaxley, David Brooke



CWLS 2015 to 2016 Executive

President

Tiffany Yaxley

Roke Technologies Ltd.
(403) 437-4065 (Preferred)
tyaxley@roke.ca

Past President

James Ablett

Exodus Directional Services
(403) 470-4888
jaymz007@gmail.com

Vice President

William Parrales, P.Eng

Nanometrics Inc.
(403) 680-9222
williamparrales@nanometrics.ca

Secretary

David Brooke

(587) 888-9419

Treasurer

Kathy Diaz, P. Geo

Wolverine Energy Services
(403) 254-9467 (Cell)
Kathydiaz1@gmail.com

Publications

Doug Kozak

Halliburton – Sperry Drilling Services
(403) 998-1966 (Preferred)
doug.kozak@shaw.ca

Publications

Manuel Aboud

Schlumberger
(403) 990-0850 (Preferred)
maboud@slb.com
manuelaboud@gmail.com

Membership

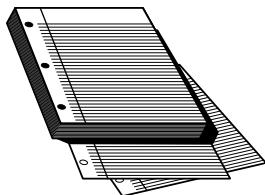
Adam Macdonald

Networth Energy Inc.
(403) 808 3795 (Cell)
adamma@telus.net

Committees

Jamie Everett

(403) 620-2403
jamesreverett@yahoo.com



Call for Papers

The CWLS is always seeking materials for publication. We are seeking both full papers and short articles for the InSite Magazine. Please share your knowledge and observations with the rest of the membership/petrophysical community.

Contact publication Co-chair:
Manuel Aboud – maboud@slb.com or
Doug Kozak – doug.kozak@halliburton.com



The President Report

It's been an "interesting" year in our industry, the CWLS executive has put in a great effort to make the most of these tough times and give back to our membership. We truly had a fantastic group of people who deserve a great deal of credit for time they took out of their very busy days to make the CWLS as strong as possible.

Giving Back in Tough Times

In the past several years we have always made a profit as an organization, this year will be the first in many we've ran a deficit. This is a hard thing to report to the membership, however being able to leverage the past profit into keeping the standard expected by our membership is something CWLS is very proud of this year.

With this in mind, CWLS put a focus on giving back by implementing a number of low cost initiatives. CWLS put on a very low cost course for new grads/students, and will have two more "free/very low" cost courses set up for 2016. CWLS started a mentorship program and are setting up to partner with the CSEG for continued mentorship workshops to gain efficiencies. CWLS has continued to invest in sponsorship of events such as; Earth Science for Society and Student events. Sponsorship dollars spent were reduced but we believe it important to continue to assist these efforts.

This year a valued member of the CWLS passed away, Winston Karoll, a long standing member and contributor to CWLS. In Winston's memory we are re-naming the Student thesis "President's award" to the "Winston Karoll" Memorial award. We received 8 student award submissions, and are pleased that we will still be contributing the same value to student awards as we have in the past.

Society Partnerships

CWLS has focused on partnering in courses, networking events, mentoring, young professional events and technical lunches with the other technical societies in town in an effort to share costs and allow members to spend their time/dollars efficiently. We are also in the process of getting the administrations of the CSPG, CSEG and SPE to build a shared calendar so our inter-society communication will help avoid repeating events and dates, again allowing technical professionals to be efficient in their development.

The SPWLA is another group we are working on building our relationship with in order to share publication material and technical resources.

Working in a team environment is something that industry is moving towards more and more. Sharing events with the other societies gives our membership the opportunity to learn more about other disciplines and for petrophysical knowledge to be shared among the technical community we all work.

2015 GeoConvention

2015 was a tough year for GeoConvention but CWLS still had a very strong technical showing with a session dedicated entirely to Petrophysical topics. The CWLS also had several volunteers work at our booth to get the word out about who we are and what we do.

The GeoConvention continues to be single-largest revenue generator for the CWLS, something which we guaranteed by signing the Joint Partnership Agreement with the Canadian Society of Petroleum Geologists and the Canadian Society of Exploration Geophysicists. The partnership forms a new entity referred to simply as GeoConvention and was in effect for the 2015 GeoConvention, which came at a good time as we were no longer required to put the upfront costs into hosting the event. Last year we did get some profit from GeoConvention, however are looking to break even for the 2016 event.

Website and Social Media

The CWLS website has been a long term project over the past 3 years and a lot has been accomplished this year. The technical expertise of Jamie Everett and tireless work of our website committee has been essential in making progress, and we still will be striving to streamline the website in the future.

Acknowledgements

On behalf of the CWLS, I also wanted to thank APEGA for their continued partnership that has gone beyond administrative assistance and office space. Anita Denton in particular has been a huge asset to our team – thank you for all of your hard work!

Closing

In closing, I again wanted to say what a privilege and honor it has been to serve as your elected president. I am so grateful to all the volunteers that have stepped up to make this past year very successful for the CWLS. The executive team was an amazing group and I would like to thank you all for your hard work over the last year. This has been a tough year for all of us and the efforts of the exec to keep the society going and really build on the CWLS' values is greatly appreciated.

To the 2016-2017 Executive, I wanted to offer my congratulations on volunteering to be a part of something very special; the friendships you will form and the networking you will have the opportunity to take advantage of, all while leading a premiere technical society will undoubtedly be very rewarding. I wish you all the best for the coming year.

Tiffany Yaxley
2015-2016 Canadian Well Logging Society President



Key Questions About Monitoring Induced Seismic Activity

Dario Baturan, Andrew Law and Sepideh Karimi

Increasingly, energy producers are faced with new regulations to mitigate risk associated with induced seismicity. Compliance typically involves using a real-time induced seismicity-monitoring (ISM) network to drive an operational traffic-light system. Most regulations specify monitoring in terms of region of interest, magnitude-based traffic light thresholds, and in some cases, event location uncertainty. Here are five key questions for energy operators to consider:

In ISM network design, how many stations are needed and where should they be located?

Science-based modeling ensures monitoring compliance in the most cost effective manner.

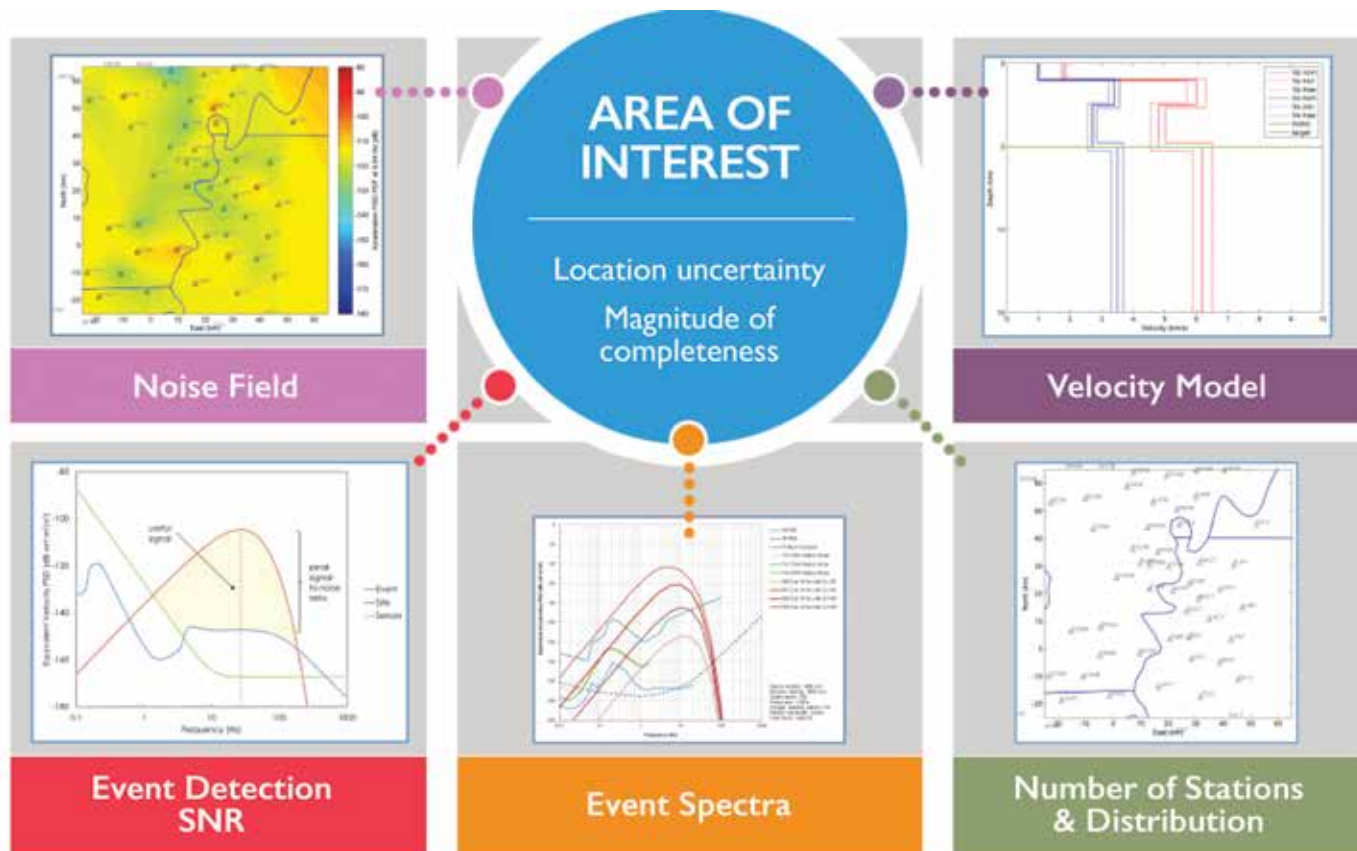
With no high-resolution earthquake catalogs for the region of interest, we model the optimal number and geographical distribution of seismic stations needed to meet the monitoring

mandate. This ensures regulatory compliance from the outset, minimizes costs, and builds robust network operation protocols into the design of the ISM networks.

As shown, the model uses hypothetical station noise and the minimum detectable magnitude for which the event signal spectra exceed the configured signal-to-noise (SNR) threshold at a minimum of four stations.

Event spectra are estimated and the minimum SNR for event detection is set to match the triggering algorithm. Epicentral and hypocentral uncertainty are estimated using a region-specific velocity model.

The hypothetical stations are then moved and their number reduced until the optimal configuration is achieved that meets desired magnitude of completeness (M_c) and location uncertainty across the entire region of interest.



Which magnitude scale should be used to drive traffic light protocols?

During recent (induced) earthquakes, reported magnitude varied depending on the magnitude scale and stations used, affecting monitoring accuracy, and therefore risking a potential shutdown order. To ensure best possible accuracy, moment magnitude (M_w), rather than local magnitude (ML) should be used. Specifically, we recommend that M_w computed using regional moment tensor full waveform inversion method be used, provided sufficient signal-to-noise ratio and a high-quality solution can be obtained. This method does not saturate, it accounts for the radiation pattern, and it minimizes site amplification effects. MW scale is related to the physical properties of the earthquake, and is the standard in microseismic monitoring networks.

Which instrumentation technology should be used?

Broadband seismometers: lower costs, smaller footprint.

ISM networks typically record events with magnitudes between M0.0 and M4.5 at epicentral distances of 2-30 kilometers. The small and rugged Trillium Compact PH broadband seismometer can sense and record the entire magnitude range at minimum cost. It has the broadband response, low self-noise and high clip level to accurately drive magnitude-based traffic

light systems and enable computations of the advanced M_w magnitudes. Because geophones saturate for larger events, they risk underestimating larger magnitudes and missing a red traffic light alert.

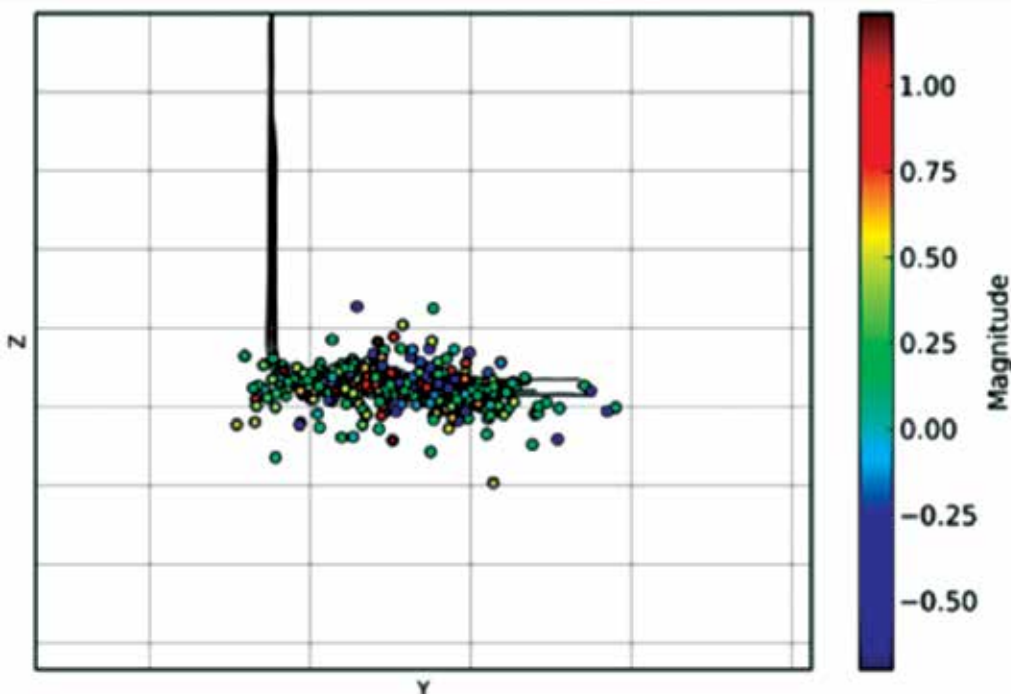
What if the network does not meet its operating mandate?

The new regulations mandate 24/7 monitoring, so it's important to understand how station outages can affect network performance (and compliance). Remotely located seismic stations can be affected by acts of nature, wildlife activity, vandalism, and communications infrastructure outages. We recommend adding redundancy in the network design, modeling the impact of each station on the ability of network to meet its mandate, and building robust monitoring protocols that include network performance-based alerts.

How else can these data be used?

In addition to driving operational alerts, ISM data sets can be used to help operators optimize completion operations, identify or refine knowledge of geological structures, estimate the direction of in-situ stress regimes, and monitor critical infrastructures and develop regional attenuation relationships for more accurate ground motion and magnitude estimates.

For more information, go to www.nanometrics.ca



Sparse Array Passive Frack Imaging



Fracture Evaluation: Height & Contribution Using FMI and Advanced Diagnostic Tools

Fractures Are Not All Equal. Find out Which Ones are Paying You Back

TGT Oil and Gas. Authored by: Dr. Fathi Shnaib

Problem Statement

Fractures, induced or natural, play a vital role in developing tight carbonate reservoirs and unconventional plays. Fracture density, orientation, and quality (open or cemented) can determine production / injection rates, and ultimate recovery. Horizontal wells completed in unconventional reservoirs, are specially cost intensive. To produce them at economical rate, and recover significant reserves, these reservoirs must be hydraulically fractured in 10, 20, 30 or more stages. The evaluation of these complex completions, the effectiveness of fractures and their contribution is most critical for a viable economic development. Conventional tools, PLT, spinner, and tracers, among others, are not capable of providing conclusive answers, partly due to their design, but, also due to complexity in completion, non-uniform low rates from individual zones, and fluid flow behind pipe. These tools have high thresholds, shallow radius of investigation, and less resolution.

Advances in technology in tools design, computing power, and innovative mathematical processing, now allow addressing these problems efficiently, effectively, and at a reasonable cost. Integrating basic wellbore measurements with reservoir flow analysis using these new tools, can provide deep and detailed answers about fractures location, orientation, density, and contribution from each zone to the overall performance.

This document discusses FMI (Formation Micro-Imager), HPT (High Precision Temp), and SNL (Spectral Noise Log) tools, field examples, and the value added from integrating acquired data with basic information from conventional tools, to get a clearer picture of fractures, in both Limestone, and unconventional, hydraulically fractured, reservoirs.

Tools

Conventional Tools

PLT's including flowmeters (spinners), temperature, and radioactive tracers, among others, has been in the field serving major and small operators for decades. Advances in drilling, completions, and tapping into unconventional reservoirs,

however, have rendered these tools inadequate to meet the mounting challenges. New tools, improved and more versatile, can now complement the conventional tools to meet these challenges and help manage reservoirs more effectively. A brief review of the typical conventional tools and a highlight of the added value from the new tools follow below:

Radioactive Tracers using Gamma ray can be effective in tracking where the injected fracturing fluid goes into the formation. They, however, stop short at that point. As Figure-1 below shows, not every interval with a high GR response corresponds to a zone that is actively producing fluid. GR have a shallow depth of investigation and the (radioactive) injected fluid can be lodged behind pipe in a non-productive zone.

PLT Spinners are very effective in pinpointing the fluid entry into a set of perforations but, they are blind beyond that point. Additionally, flowing, or injecting rates can be too low to be detected by the relatively high threshold of these tools. These tools won't help much either, in dual completion.

Old Temperature Tools had a slow response and poor resolution to pick up fluid movement behind pipe, let alone in dual or multi-barrier completion. The introduction of a new tool like HPT, with 0.2 degrees C resolution and fast response, can provide a highly accurate temperature profile along the wellbore. Supplementing this with TERMOSIM, temperature simulation, will enable quantifying production or injection rate without running any spinners.

Integrating data from the above conventional tools with measurements from new tools, will provide a powerful combination to meet most challenges in the modern field operations.

FMI Compared to all similar tools in the market, FMI yields the most detailed data, measuring all natural and induced microscale changes that take place in the rock texture of the reservoir. The tool generates a high-resolution image of the wellbore wall, covering 80% of the target area in 21.25 cm (8.5") hole. Micro-conductivity electrodes can see as far as about 12.5 mm (0.5") into the formation, and are capable of recognising conductivity anomalies that are within effective resolution of the tool (5 mm or 0.2"). Images from FMI are core-like



wellbore images based on high-resolution electrical resistivity data. Small FMI data details can be used for identification of different types of fractures, faults, and textural features.

FMI alone, however, is only effective for describing the wellbore, and near wellbore initial conditions. It will not be of much use to detect subsequent changes to a natural fracture system or to fractures induced (HF stimulation), or damage to existing fractures.

Therefore, additional methods of behind-casing analysis are required to obtain reliable and updated data on the reservoir flow regime. To achieve this, HPT-SNL surveys are carried out and the results are integrated with FMI and other data to evaluate fractures and reservoir performance.

HPT and Temperature Modelling

Temperature logging is one of the oldest diagnostic tools in the oil field. Measurements of variation in temperature along the wellbore, were used to locate top of cement, entry of hot reservoir fluid, and injected water exit into the reservoir. Improved tool design, however, are now more sensitive, have much faster response, and higher resolution.

Furthermore, TERMOSIM, a highly sophisticated mathematical modelling software can be used to simulate and history match temperature profiles obtained from tools such as the HPT. This allows engineers to quantify rates too low to measure by other tools, like spinners, and describe fluid flow behind pipe even under static conditions. Integrating this data with data from FMI, tracers, and SNL provides a powerful tool to evaluate fracture height, fracture quality, and allocate production to active fractures.

SNL Tool

Spectral Noise Logging is an advance technique used for well integrity control, identification of producing and injecting reservoir units, and reservoir characterisation. Fluid and gas flows generate noise due to vibration produced by the rock matrix and well completion components. Noise intensity would go up linearly as fluid/gas rate increases. However, the noise spectrum composition would depend on the type of medium through which fluid is flowing rather than on the flow type or rate.

An analysis of acoustic noise recorded in a wide frequency range will help to identify active reservoir zones, casing and tubing leaks, active perforations, behind-casing channelling, and distinguish between matrix and fracture flows. Application of Spectral Noise Drift (SND) technique (wavelet thresholding algorithm) to extract reservoir noise enables reliable rejection of noises with dissimilar characteristics because their contribution

to wavelet factors of considered modes are small and could be filtered by the derived threshold value. When a noise spectrum is analysed, it should be taken into account that as the flow induced by a pressure drawdown is forced through a large-diameter hole, a low-frequency noise is generated, and, if the hole is small, the noise will be in a higher frequency range. By applying the same principle in an attempt to define the flow pattern, we will see that as the fluid moves through the low-permeability units, a high-frequency noise signal is generated. Broadly speaking, when the fluid flows through a fracture (natural or induced) it normally generates noise of about 2 kHz or lower, while in a porous reservoir of medium and high permeability the frequency will be in 2-20 kHz range and above 20 kHz in a low-permeability reservoir.

Conclusions

1. New advances in drilling and completion technology have created new challenges in reservoir evaluation and production management.
2. Old conventional Production logging tools, although still useful for what they were designed for, fall short of meeting the new challenges.
3. Tracers and Gamma Ray logs can detect where the frac fluid goes, but their response correlates poorly with reservoir behavior.
4. However, to get maximum value, conventional tools data and data obtained from new tools like HPT and SNL, must be integrated. This will be the best way to overcome the new challenges and provide effective means to manage field operations and reservoirs.

Examples – Field Cases

To illustrate the advantage and added value of integrating FMI data and data obtained from HPT and SNL, the following examples are shown on the following pages:

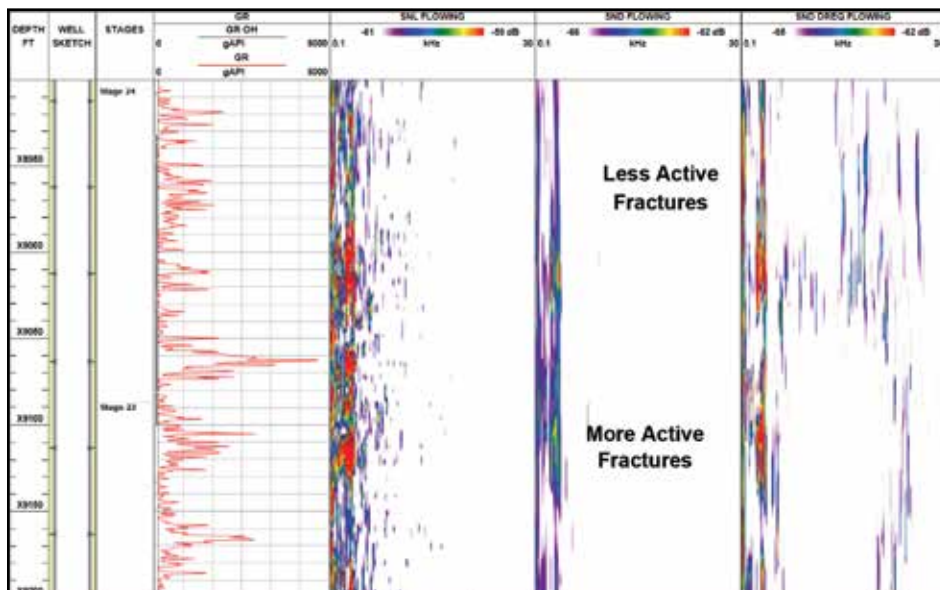
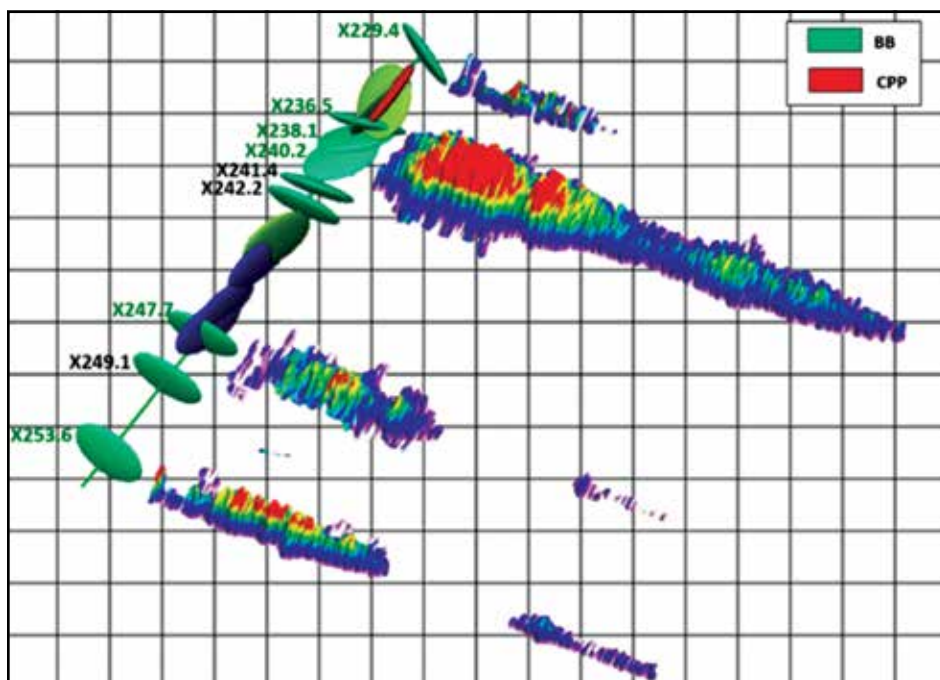


Figure 1 is showing that GR (Tracer Tacking) does not always correlate with active zones



Depth color:
 • Cemented fracture
 • Open fracture

Figure 2 3D overview (Interval x229-x254) showing excellent correlation between open fractures (green figures) from FMI and SND flowing zones. Meantime, cemented fractures (marked in black) show little or no flow.

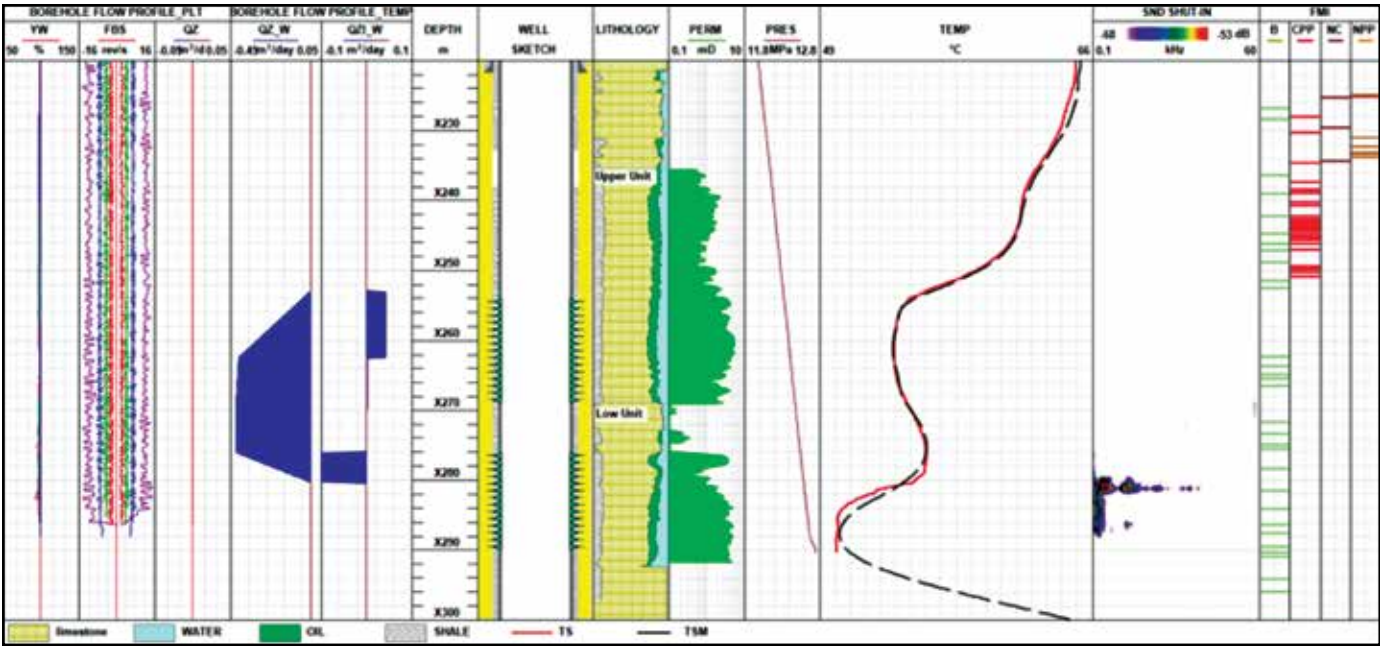


Figure 3 is showing flow from Spinner data on the left matching flow obtained from TERMSIM. The figure also shows that the lower set of perms are flowing into the wellbore under SHUT-IN condition, indicating a lateral flow. This flow is clearly shown on the SNL panel as partly from fracture (low frequency) and from matrix (higher frequency).... The flow is occurring across a heavily fractured zone shown by FMI. TERMSIM shows the lateral flow to go up behind pipe and into the upper set of perms, where FMI shows no fractures.

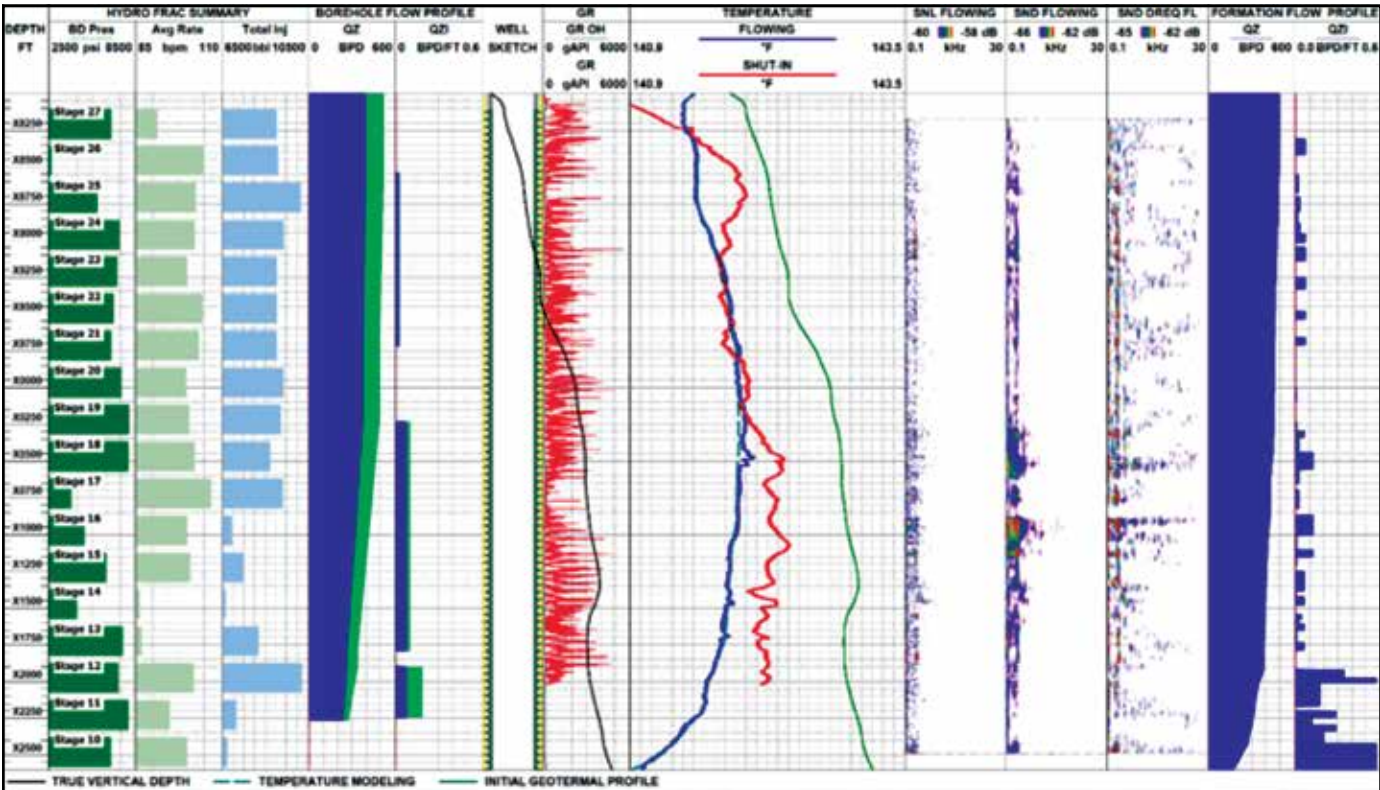


Figure 4 Integrated logging results: PLT shows good correlation with SNL except in stages 26&27. Radioactive tracers/GR is pretty much smeared over the entire interval, but with good correlation in spots like Stages 16&17 (low GR and low rate on SNL). HPT and SNL show that over 60% of the completion is contributing to the flow, while the GR tracer indicates that over 90% of the interval was contacted by fracturing fluid.

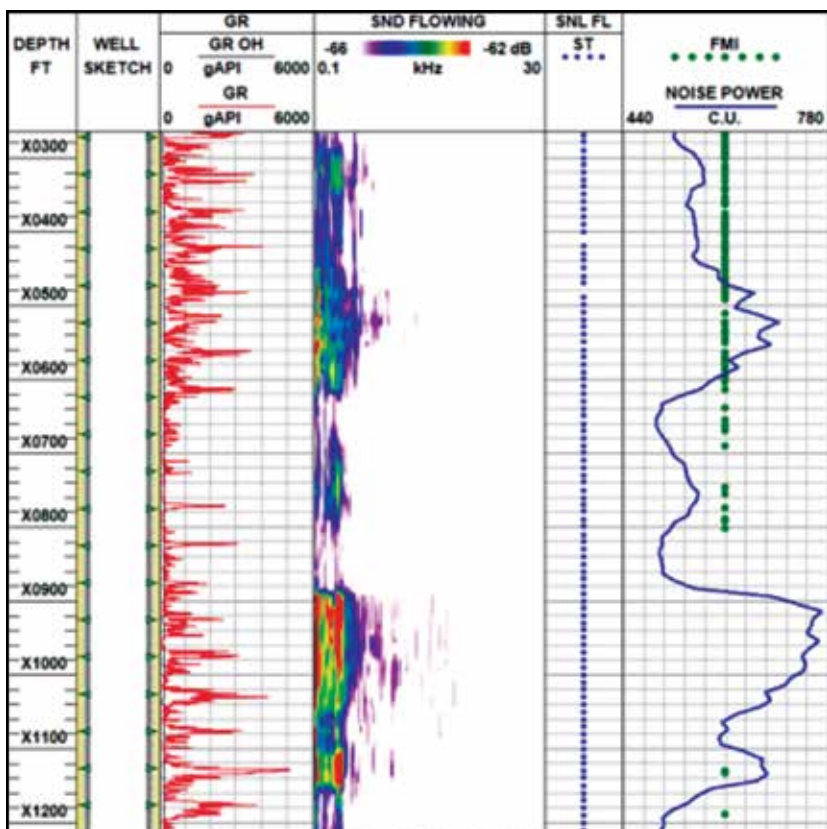


Figure 5 Shows a good correlation between FMI fractured zones and active flow- e.g. X0720 and x0800 and these were natural fractures that got stimulated. In the interval x0900 to x-1080 no natural fractures existed before the well was hydraulically frace'd.

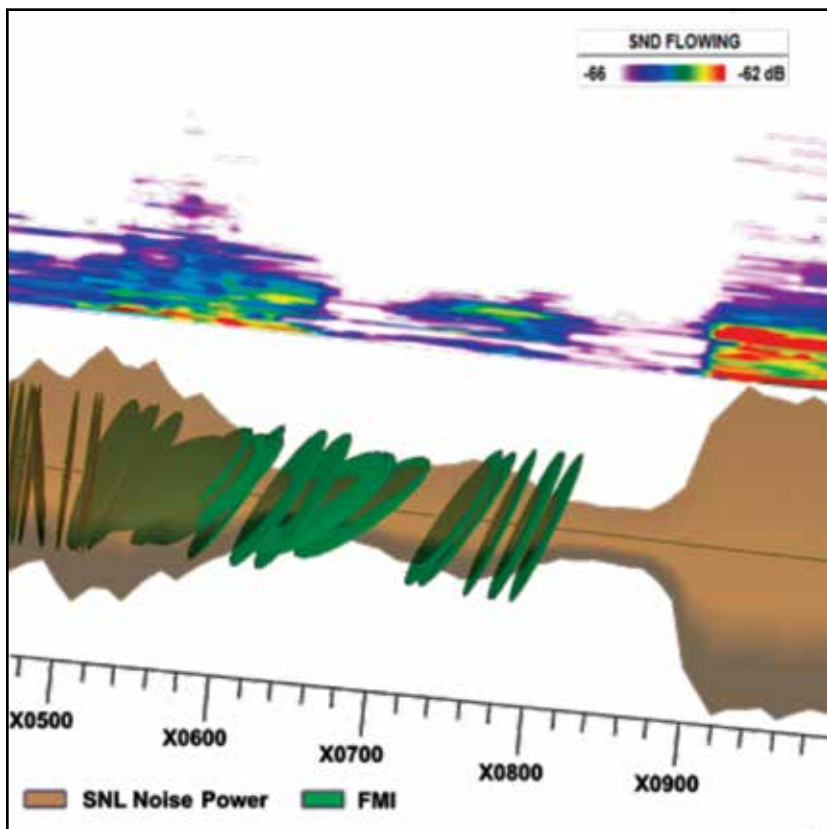


Figure 5A is a 3D illustration of the above

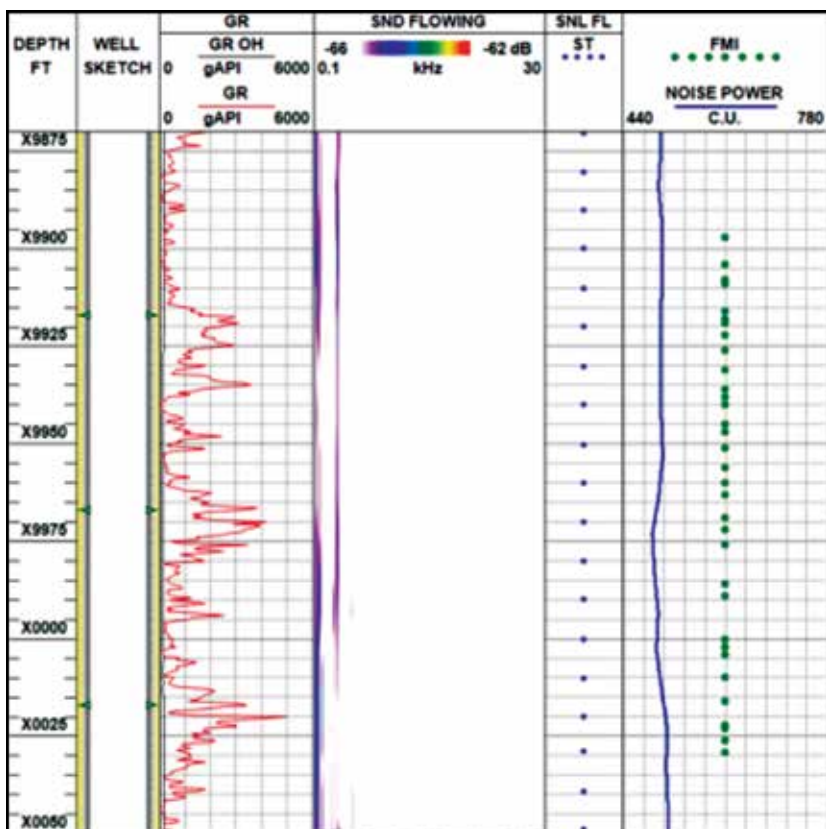


Figure 6 shows that although this interval was naturally fractured and then it was stimulated but shows very little flow, in spite of the fact that the GR/tracer log confirms that it was stimulated.

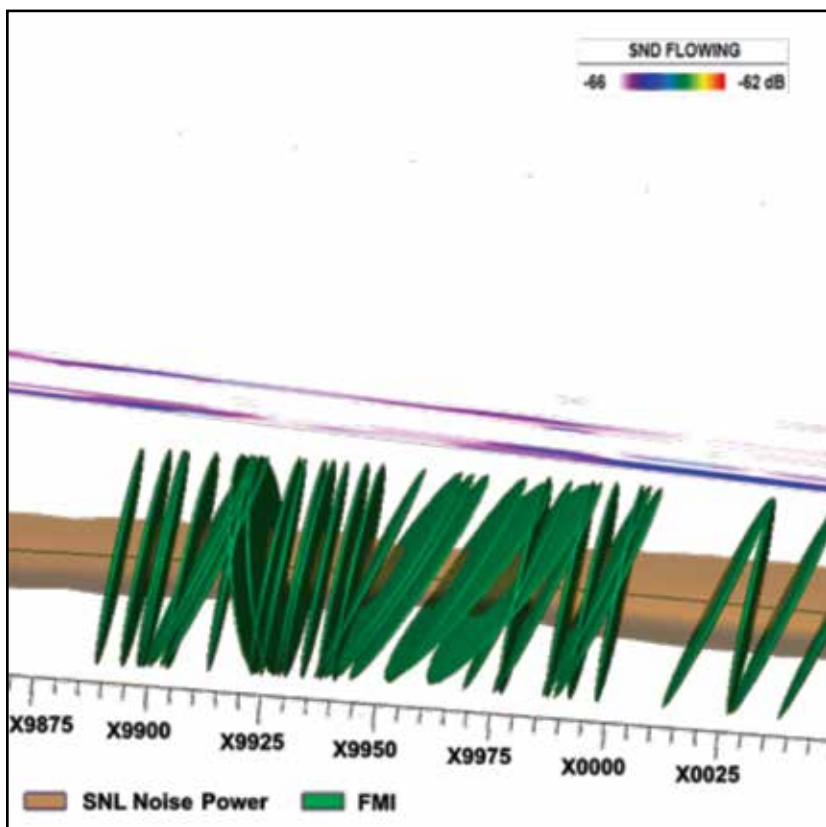


Figure 6A is a 3D illustration of the above



Delineation of thermally altered zones in SAGD producer wells through resistivity characterization using LWD azimuthal propagation tool

Anand Gupta and Alan D. Cull, Halliburton Sperry Canada
Ian Theunissen P. Geo & Jim Koch P. Eng, Statoil Canada

Summary

In this paper, an attempt is made to study and characterize thermally altered zones within a bitumen reservoir in terms of varying resistivities reflecting the oil saturation variation due to active steam injection across the horizontal well bore. Resistivity profiles generated from real-time ADR (Azimuthal Deep Resistivity tool) data is compared with oil saturation models composed prior to drilling of two horizontal wells. Applicability of LWD (logging while drilling) azimuthal propagation tool's data is discussed with reference to real-time data from two geosteered second stage SAGD producer wells.

Introduction

In an era of ever increasing emphasis on maximizing oil recovery, an advanced geosteering approach is demonstrated to have definitive advantages. Most commonly, geosteering practices are used for optimal well placement to increase hydrocarbon recovery. Applications of geosteering tools and software in other areas, apart from placing the well, are still under-explored. Statoil Canada Ltd has only recently realized the potential for optimizing startup strategies by effectively delineating thermally altered zones in geosteered second stage SAGD wells.

LWD azimuthal resistivity offers the ability to investigate several meters beyond the well bore. Changes in the electromagnetic field from transmitter to receiver are due to the resistivity of the surrounding lithology. Resistivity is also a key component to Archie's equation for water saturation, providing a strong correlation between resistivity and oil saturation.

Combining resistivity readings from different depths of investigation, as well as a comparison of raw phase and attenuation values provides a means to indicate oil saturation variation due to steam infiltration across the horizontal SAGD well bore. Resistivity profile generated from real-time data is compared with modified oil saturation log composed prior to drilling. Issues with such an approach are addressed and applicability of LWD azimuthal propagation tool's data is discussed with reference to real-time data from two geosteered second stage SAGD producer wells.

Theory and/or Method

In 2014 and 2015 a series of second stage SAGD producer wells were drilled in a mature heavy oil field for Statoil Canada Ltd in Western Canadian Sedimentary Basin using LWD azimuthal propagation tool and geosteering service (well placement). SAGD producer and injector well pairs were initially drilled within the area of interest between September 2008 and December 2009. After 4.5 years of production, the second stage producer wells are planned within the same area for the second phase of enhanced oil recovery. Objectives for drilling the horizontal second stage wells are (1) placing the well 4m above the base to increase the volume of recoverable bitumen and (2) demarcating the thermally affected areas.

Azimuthal deep resistivity sensor is used as a part of BHA (bottom hole assembly) in this study while drilling four wells. This azimuthal wave propagation tool is designed to detect resistivity changes within a few meters of the ADR tool (Bittar M., et al. 2007). Recorded changes in EM wave properties are modeled to reflect variation in the resistivity of the formations around the well bore (Pitcher J. and Bittar M., et al., 2011). Three spacings (between transmitter and receivers) viz. 112", 48" and 16" are used with tool's frequencies at 500kHz, 125kHz and 2MHz for readings at different depth of investigations.

Prior to drilling a conceptual model of the altered reservoir is created from the most recent saturation logs from nearby observation wells. Furthermore, pre-steam offset well logs are also available to establish a baseline for original reservoir properties. While drilling, a cross section profile for each well is created from real-time azimuthal resistivity data (Figure 1a) and is modelled with the help of geo-steering software. The resistivity variations are used to interpret the thermally altered zones in the reservoir along the well bore. Real-time temperature data from onboard the ADR tool sensor is also used to confirm the demarcated thermally affected areas.

IHS (Inclined Heterolithic Stratification) in McMurray formation may create barriers for steam movement and so affect the production from a single horizontal well at different zones.

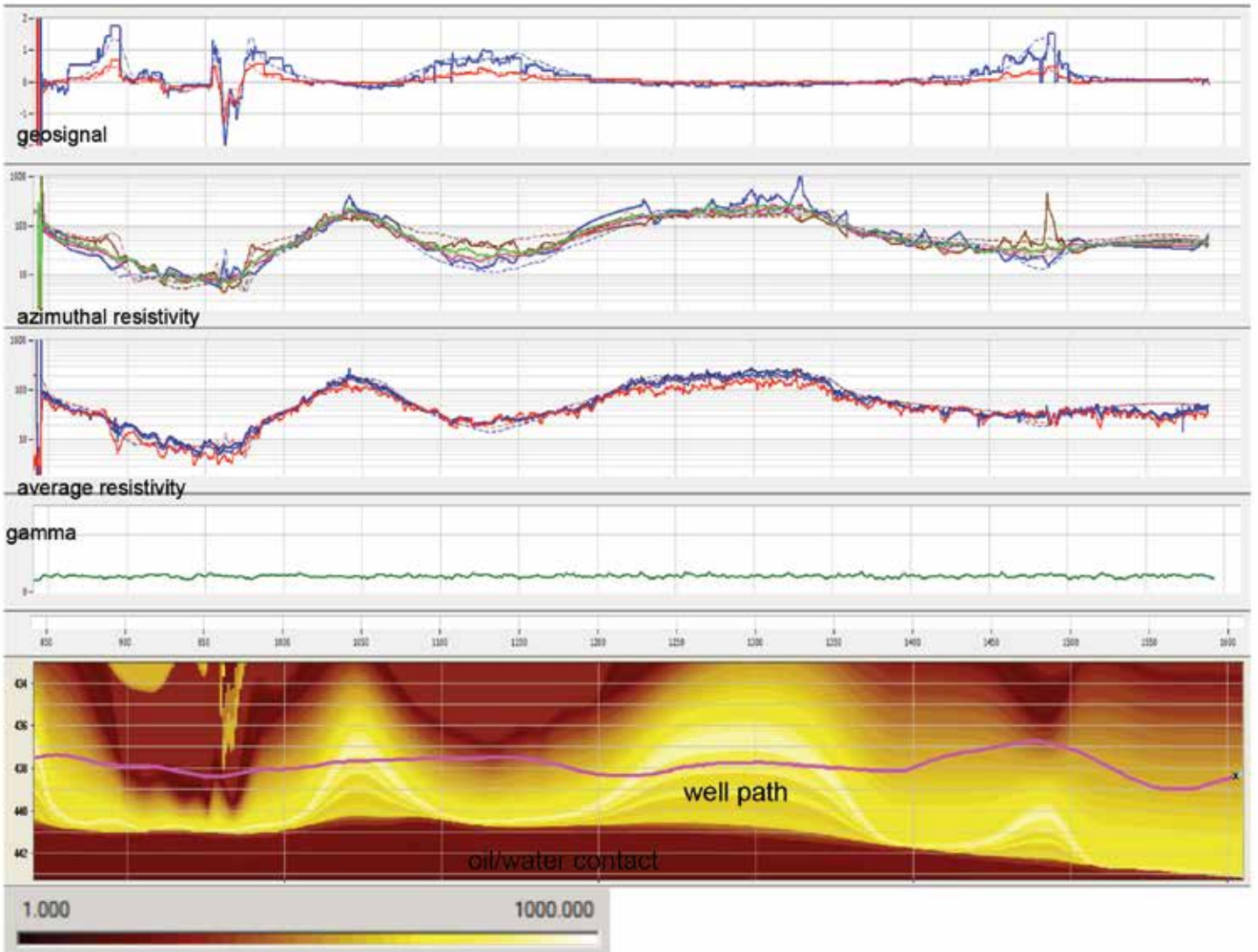


Figure 1a: Data used in modeling the resistivity within 5m of the well bore. Darker regions represent areas of low resistivity. The dark area several meters below the well path represents the oil/water contact while the darker regions around and over the well path reflect low resistivity are associated with thermally altered zones.

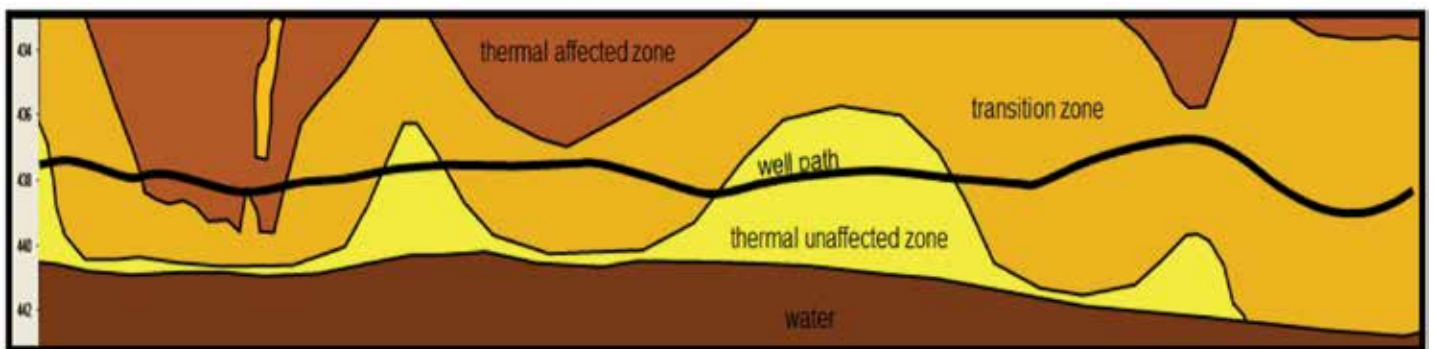


Figure 1b: Schematic diagram indicating the Azimuthal Deep Resistivity tool's and Strataster Geosteering Service's ability to map resistivity zones around the well bore, and correlate this to the thermal effects from the surrounding SAGD well pairs.



In this study, an attempt is made to correlate the shape of resistivity profile with heterogeneity of the rock structure within the reservoir. This plays critical role in understanding the extent of steam saturation / propogation.

To maintain minimum 4m TVD difference from the oil-water contact, a combined proactive geosteering approach is used. This is based on the combination of azimuthal resistivity, gamma ray, real time petrophysical information and a 3-D interactive correlation software. These data sets allows for the modeling of the geology in the area and the theoretical response of the tool based on offset wells' data. Derivations from the deepest reading sensor, Geosignal (112" at 500kHz), is used to estimate the distance to bed boundary quantitatively. Theoretically a low resistivity response approaching from above may be indicative of a thermally altered zone. Conversely the same response approaching from below may indicate an approaching water boundary. Each response would dictate a unique geosteering corrective action.

Examples

The objective is to map and determine the effects of the thermal activity from the surrounding SAGD well pair and then delineate thermal unaffected zones (Figure 1b). The thermal unaffected zone should reflect the characteristics of the original in place bitumen. The thermal affected zone can represent (1) a zone of mobile bitumen, (2) a decrease in bitumen saturation, (3) an increase in temperature, and/or (4) an increase in steam saturation. The transition zone is reflective of the heat gradient between these two main zones.

Conclusions

Azimuthal deep resistivity tool and its petrophysical interpretation greatly enhance the ability of well placement and improve the understanding of the reservoir. Thermally altered zones near a second stage SAGD horizontal producer well can be delineated along with an estimate of reservoir quality.



RESPONSIBLE ENERGY DEVELOPMENT

At Nexen, we are focused on safely and responsibly delivering energy to a world that needs it. We apply technology and innovation to minimize our impact on the environment.

By partnering with our stakeholders, we identify and implement business solutions which create mutual benefits.



www.nexencnooltd.com



Understanding the distribution of these different zones along the horizontal section of the wellbore can aid in optimizing the startup strategy and minimize time to bring a well into production phase. Furthermore, this information can be used to determine the feasibility of a second phase drilling campaign, design the liner configuration and/or help determine the best method of production.

Acknowledgements

The authors thank Statoil Canada for the support and permission to present this work.

References

Bittar, M., Klein, J., Beste, R., Hu G., Wu M., Pitcher J., Golla C., Althoff G., Sitka M., Minosyan V. and Paulk M., 2007. A New Azimuthal Deep-Reading Resistivity Tool for Geosteering and Advanced Formation Evaluation. Paper SPE

109971 presented at SPE Annual Technical Conference and Exhibition, Anaheim, California, USA, 1-14 November 2007.

Pitcher J., Bittar M., Hinz D., Knutson C. and Cook R., 2011. Interpreting Azimuthal Propagation Resistivity: A Paradigm Shift. Paper SPE 143303 presented at SPE Annual Conference and Exhibition, Vienna, Austria, 23-26 May 2011.

Strobl, R., 2014. Conductive Heating in Steam Assisted Gravity Drainage (SAGD) for Thermal Recovery and Production. Presentation at Slugging It Out XXII, CHOA, Calgary, Canada, 1 April 2014.

GeoConvention 2016

GeoConvention
Calgary - Canada - March 7-11 **2016**



OPTIMIZING RESOURCES

With low commodity prices and an ever-changing economic and business environment, it is imperative that the industry optimize the way in which it operates. Whether enhancing recovery methods, finding the optimal path for a horizontal well or maximizing the return of capital employed, Optimizing Resources, the theme for GeoConvention 2016, is key to success.

Please join us and contribute as speaker, exhibitor or sponsor



**GeoConvention 2016:
March 7 – 11**

In recognizing the business environment which we are operating in, **GeoConvention is pleased to offer heavily discounted delegate rates for the 2016 program.**

New for our 2016 program, in addition to the technical program and exhibit floor at the Convention Centre, **we will be hosting an offsite component, including panel discussions, workshops and a mini core conference at the Lake Louise Inn – check out www.geoconvention.com for details.**

**REGISTRATION
NOW OPEN**

www.geoconvention.com



Three Methods for Log-Derived Mineralogy: Part Three... Petrophysics Designed to Honour Core: at Work in the Montney Formation

R.V. Everett, Robert V. Everett Petrophysics Inc.

Overview of Petrophysics

This report discusses details of the petrophysical work in one well in the distal region of the Montney Formation in Northeastern BC, which was presented as an Abstract, Ref. 12. There are two logging runs in this well, recorded in separate holes. The vertical section was logged by Schlumberger (SLB), and the deviated hole logged by Baker Hughes (BH). Cuttings and cores were collected from the straight hole. We exploited the opportunity to use neutron spectroscopy and magnetic resonance logs from two service companies with cuttings analyzed with QemScan and Furgo. Additionally routine core analysis was exploited using interpretation models developed specifically to use elements and core/cuttings minerals. The procedure found that tools from both service companies' worked well to provide mineralogy that matched the core/cuttings results.

In previous InSite Articles, we described the basics of the interpretation method in Ref. 8 and the predicted model applied to wells that did not have the ECS, Ref 13. A summary of the techniques used to date is listed in Appendix H.

The third method of interpretation uses a process called Robust Elm (Ref. 1, 2) developed by Dr. Eric Eslinger for his Geological Analysis by Maximum Likelihood Systems (GAMLS) and modified by Robert Everett to include the free fluid index of nuclear magnetic resonance. In Robust Elm's methodology, the inputs for each well are the clustered lithology, recorded neutron, resistivity, GR, neutron spectroscopy elements and cutting's mineralogy. Constraining all inputs provides the most likely output-minerals to be compared to the cutting's mineralogy, total organic carbon (TOC) and grain density, as well as routine core analysis (RCA) porosity and permeability. The computed logs compared closely to the cutting's grain density and mineralogy over the Montney but had much lower grain density and different mineralogy than the cuttings over the Doig. The mineralogy is illustrated by the cutting's quartz: the quartz on the cuttings was lower than the quartz on the interpretation in the Doig, but both were very close in the Montney. The LAS file also contained an interpretation over the Montney section of the Baker hole, providing a mineralogy that agreed with the new interpretation as well as the cutting's mineralogy.

Executive Summary

Overall Summary

The vertical hole logged by SLB used a laterolog array for resistivity, epithermal and thermal neutron logs, dual barite-corrected density logs, elemental capture spectroscopy (LithoScanner™) and nuclear magnetic resonance (CMR-PLUSTM). A deviated sidetrack logged by BH used a laterolog array, thermal neutron logs, dual density log, elemental spectroscopy (FLEXTM) and nuclear magnetic resonance (MREXTM) as well as an acoustic array (XMACTM). The SLB run covered the Doig, Montney and Belloy. The BH run did not go as far down to cover the Belloy. As the original data was not initially available, an edited LAS file containing the two runs with missing information about the well location etc. was used. Once the data was separated with the assistance of Ramdane Bouchou (BH) and Rob Badry (formerly SLB) both sets of data agreed with core over the Montney section but not with the Doig section. The inputs to the interpretation were the conventional well logs, a clustered lithology of the well logs, the nuclear spectroscopy and nuclear magnetic resonance logs and the cutting's mineralogy by SGS. Later, a cuttings file by Furgo in volume % was also available, as was X-Ray Diffraction mineralogy. The LAS file also contained an interpretation (author unknown) over the Montney section of the BH hole. The core/cuttings mineralogy agreed with both the new and the anonymous interpretation. Mineralogy of the Montney formation changes from well to well, especially with respect to clay content and calcite/dolomite fractions.

Final products

1. Simplified plots of interpretation (plots are defined as simplified when they contain pertinent curves but leave out the curves testing validity)
2. Detailed plots of interpretation, including the validation curves
3. LAS files of interpretation
4. Tops and summaries of net pay etc., for the interpretation
5. This report



Summary Presentation of Work

1. The purpose of the petrophysical interpretation is to provide net pay, net porous and gross pay as well as Sw and porosity to provide hydrocarbon pore volume.
2. First, calculations for the above are done using the recorded density log. To compensate for washouts, corrections would normally be applied as explained in Appendix C, but were not necessary for these holes. A method outlined by Barry Johnson (pers. com. during May School on Petrophysics with Spectroscopy) decides which of the two densities to use in the interpretation, wherein the density that has the lowest density correction is used. The PEF may or may not be recorded on this same density orientation, so do a histogram and pick the lowest PEF. The higher PEF will be affected by barite.
3. The wells had complete data, with capture spectroscopy for elements and nuclear magnetic resonance for free fluid. A natural GR spectroscopy (SLT, NGT) was also available for each hole. The SLB logs were run on 0.0254 m (12 samples per foot, high resolution).
4. In summary, we provided results from an enhanced data set.
5. Consequently, optimum logs and interpretation was possible in this stable hole.

Petrophysical Summary

As outlined in Part Two (Ref. 13) a log interpretation method, not commonly available, is designed to incorporate and be calibrated by core.

Our interpretation starts with the most basic inputs that can be correlated to core measurements every step of the interpretation. For example, we start with predictions of the elements, (Ca, Fe, Si, and S) from nuclear spectroscopy and measured natural gamma spectroscopy U, and K & Th.

We invoke an element to mineral model from the program "Petrophysics Designed to Honour Core" to derive the common minerals from the input elements. While this may seem an obvious strategy, there are more unknowns than knowns involved. It is accomplished by a normalization procedure using the elements as constraints. Alternatively, a normalization procedure has been developed using the core minerals as constraints in the Geological Analysis by Maximum Likelihood Systems (GAMLS) program.

Derived-mineralogy attributes are used to derive cation exchange capacity, grain density and permeability and were compared to core porosity and permeability.

Introduction

Why involve mineralogy? We use mineral attributes such as cation exchange capacity, grain density and surface area to compute Sw, porosity and permeability. Analysis will be complete if diagenesis does not modify the calculated attributes (CEC, Perm, m, n) from our model values. Consequently, comparisons to GRI or RCA core measurements are necessary. From these predicted elements, mineralogy provides a complex interpretation of porosity, water saturation and permeability. We use a flexible interpretation program to perform checks and balances at each step of the process. The final criteria for net pay flags is given in Appendix B.

We had this information:

A pressure gradient from offset wells was about 0.52 psi/ft. For the temperature, we used $0.0198 * \text{depth} + 42.08$ in feet and Fahrenheit degrees. The Rw used was derived from the SP and Rmf of 0.387@20C plus calibrated to Rw from the catalog of 0.1@25C as outlined in Ref. 8. The multiplier used on the BVW value for irreducible water was 1.2.

Method

As outlined in Ref. 13 our method is to:

- a) Prepare reliable data before entering the calculation programs.
- b) Correct for washouts affecting the density: the hole was in good shape as evidenced by the density correction, so correction was not subsequently made before the final pass but is described in Appendix C.
- c) Predict missing log curves; all curves were present for this data set.
- d) Determine Rw from the SP. The Rw derived from the SP was calibrated. The SP fluctuations allowed propagation of the Rw to the top of the well. I outline this method in the spring 2014 CWLS 'Insite' magazine, available on the CWLS website (Ref. 8).
- e) Calculate the total organic carbon (TOC). The empirical calibration for TOC was $5 * (\text{Log}_{10}(0.25 * \text{HURA}_P) + 1.85)$ to give a result in weight percent. We modified this result in a cluster to better conform to core TOC.



Calculations in the program

As outlined in Ref. 13,

1. Solve for clastics, carbonates, and clays respectively using log elements from the ECS/LithoScanner/Flex curves (Al, Ca, Fe, Si, S and potassium [from the natural GR]).
2. Normalize by constraining with log elements and measured GR spectroscopy (K, U, Th), to convert the Si & K to quartz, kspar, plagioclase and muscovite; Ca to dolomite, calcite and anhydrite (via sulphur); Si, Al, K and Fe to illite, smectite (none), kaolinite and chlorite. The clay was primarily illite.
3. A note on the Robust Element to Mineral model (Ref. 2). The method uses three inputs:

The first input is a cluster that uses any preferred log combination. For this well we used density, neutron and gamma ray. The number of modes desired is also a variable input. We chose 15 modes in deference to Dr. Michael Herron who said that most sedimentary formations usually have only 13 minerals that are dominant (pers. Com. about 1985).

The second input is mineralogy. We chose the QemScan minerals run by SGS. The program automatically allocates the mineralogy to the 15 modes, so now we have core/cutting mineralogy calibrated to the modes.

The third input is the elemental capture spectroscopy elements. The program automatically assigns these elements to the modes.

The result is a triple constraint on the log calculation of mineralogy.

4. Solve for porosity and permeability using the Herron formulas (Ref 3) involving the log elements and the calculated carbonate, clay and siliclastics groups.
5. Solve for Sw and provide estimates of irreducible (Swirr) and minimum water saturation (SW_DS_GAS_ECS) to estimate if water will be produced. The formulas used for Swirr were from Coates and Timur as noted in the Patent publication number CA2463058, (Ref. 15) and those used for minimum water saturation were modified from those developed by John Nieto (Ref. 14).

Here are the steps for the Sw calculation. All steps are iteratively performed for 10 iterations:

- The saturation equation used is called a Dual Water Equation, from the paper by Chris Clavier et al, (Ref 5)

- The components of the equation are:

m_zero , which is the cementation factor, dependent on m^* (m_star), the Waxman-Smits cementation factor (Ref. 15):

IF $((m_star < 2.0356) , (m_star / (0.1256 * m_star + 0.7781)) , ((m_star / (0.3764 * m_star + 0.2694))))$, where

$m_star = (1.653 + (0.0818 * (Surface\ area * RHOG) ^ 0.5))$, where

Surface area (SO) = sum of SO of each mineral

$n_zero = tortuosity\ factor = m_zero$

CEC = cation exchange capacity of each mineral summed

TPOR = total porosity from the density and grain density derived from elements

Rw_SP = the formation water resistivity derived from the Rmf and SP

Rt = assumed from the deep reading resistivity

6. Create flags for net pay (PHIE > 6% & Hydrocarbons), net porous (PHIE > 6%) and gross porous (PHIE > 3%) zones. See the Sw-porosity plot Appendix D.

Discussion

This report includes detailed computations in Appendix A. NMR logs were available for the holes studied. Elemental Spectroscopy was also. The mineralogy result was about 1/3 quartz plus 1/3 calcite and 1/3 dolomite in the cleaner sections. Clays replaced the matrix minerals in the shaly sections. The interpretation provided Sw, k, Por. The maximum Sw agrees with a value of $1.2 * Sw_DS_Gas_standard$. This mult $* Sw_DS_Gas$ can therefore be used as an irreducible Sw, to yield a BVW_irr of about $1.2 * 0.0150$ to $1.2 * 0.0170$. On the Appendix D look at Sw vs. porosity.

See Plot (Appendix A) entire zone, showing the Robust Elm result first, followed by, in Appendix D, the ECS result and the Baker Hughes result. [Note, Robust Elm is run separately and its results are added to the ECS inputs for a combined ECS-R_ELM output via the PDHC [ECS] program. The purpose of combining them is for conformance in reporting summaries].

Net Pay Criteria is outlined in Appendix B.

Corrected log bulk density methodology is outlined in Appendix C.

The minerals and SW vs. Porosity are in Appendix D.



An explanation of the curve coding for Sw and porosity is in Appendix E & F.

A 'Quick Look' model is presented in Appendix G.

A summary of the techniques used is in Appendix H.

Results

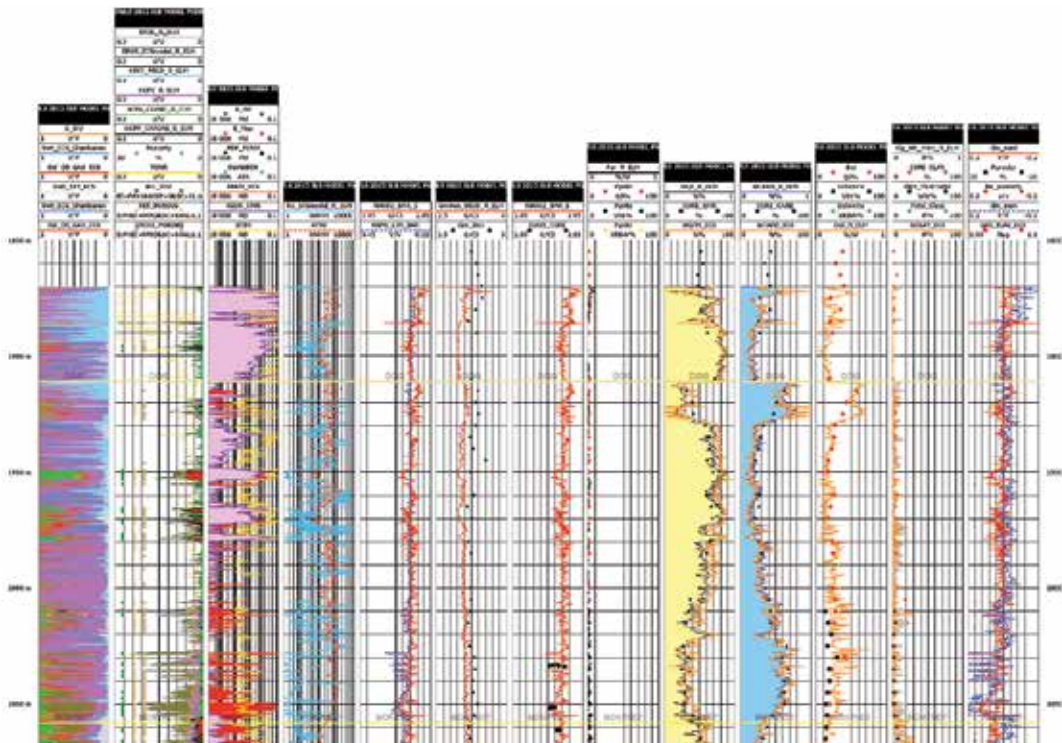
The results of the Model are in Appendix A.

Everything turned out as well as could be expected considering the stable hole and complete logs and cuttings/core analyses.

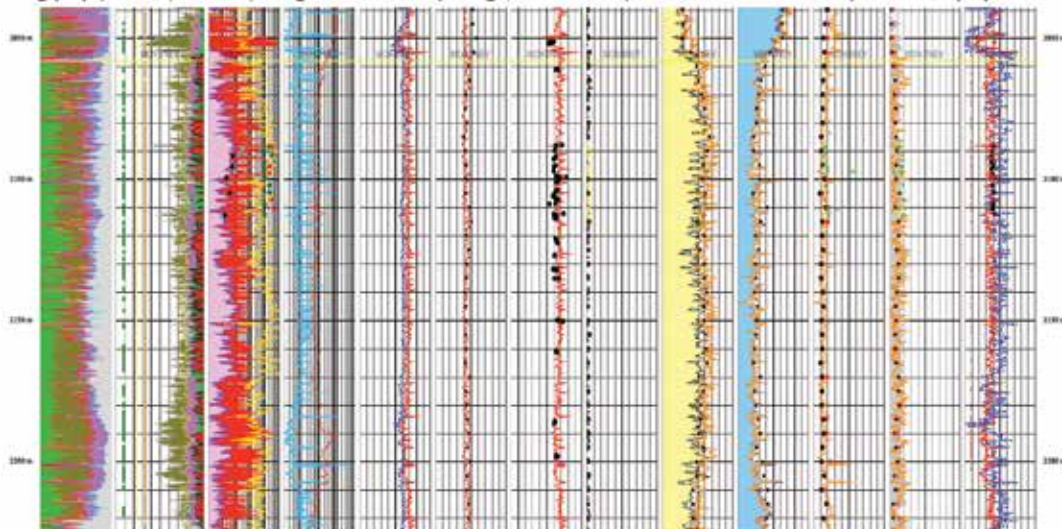
Conclusions

When one uses log elements as well as nuclear magnetic resonance, the results are excellent. The Quick Look plots in Appendix G illustrate the value of the logged elements and NMR.

The zones-of-interest are below. Normally the 0.0254 m/step is preferable to acquire and process the data. A zoom of 232% may be necessary to view the scales.

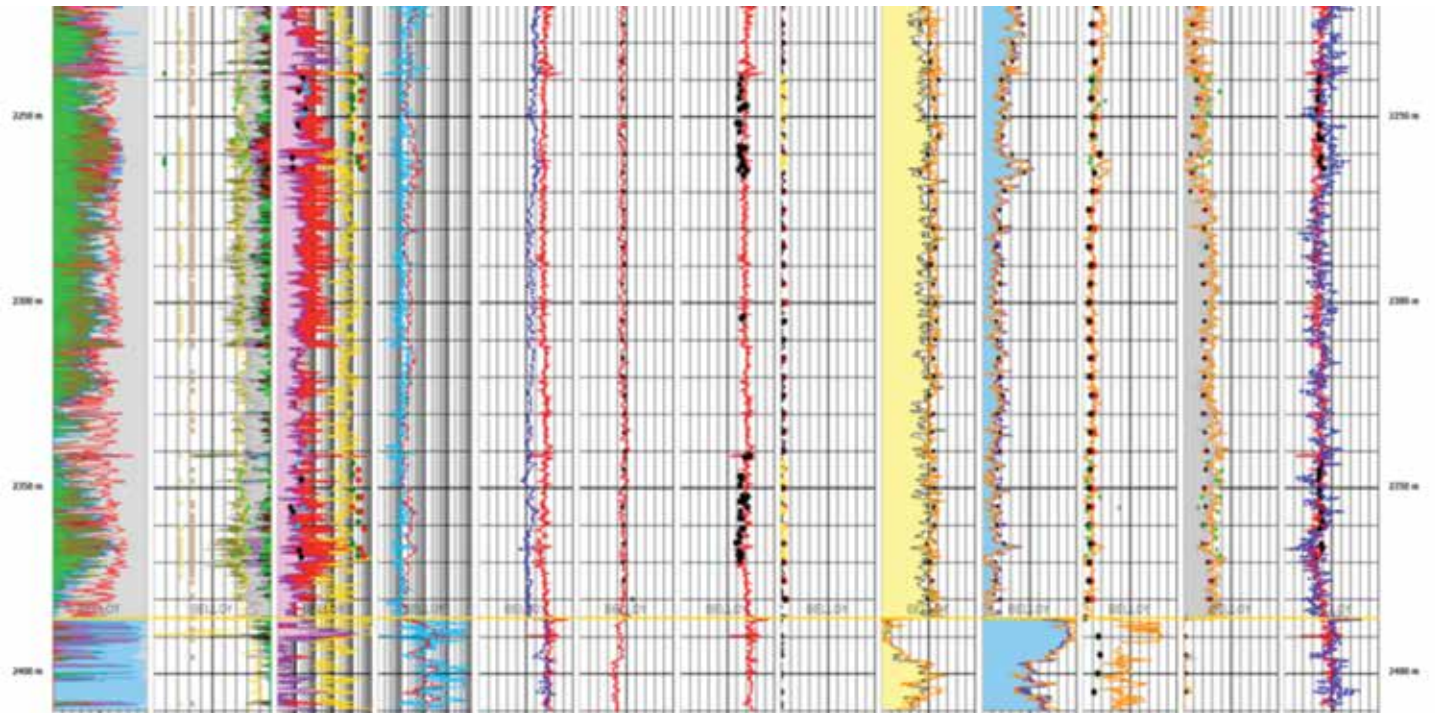


Doig pay (above) is low (see green 'Net Pay' flags, Track Two). Almost all Montney below is pay.





Montney pay zone is shown above. Montney lower zone and Belloy are shown below and have no pay.



Summary based on Hi Res 0.0254 data.

TOPS & SUMMARY		WELL: CSPG CWLS MAY 2015 FDATE: 2015-02-01 14:46:18		STRT: 1870 STOP: 2410											
Formation Name	Top	Bottom	Interval	NET_PAY_PHE+PAY1&HCPV	Porous_PHE+PAY2	Gross_PHE+PAY3	Sw_avg & Net	Sw_avg & Porous	Sw_avg & Gross	TPOR_avg & Net	TPOR_avg & Porous	TPOR_avg & Gross	HCPV		
TOP OF WELL	1870	1911	41	0.55	0.9	1.375	0.07990852	0.06790685	0.096030069	0.06648089	0.095270677	0.088624524	0.015164421		
DOG	1911	2030.12987	119.12987	8.05	12.4	20.25	0.080475564	0.211137335	0.250818819	0.06694231	0.062218927	0.052781125	0.107717848		
MS4	2030.12987	2055.06494	24.93507	6.7	11	14.15	0.045108199	0.119152855	0.144668956	0.08882204	0.075552078	0.06687495	0.074159943		
TS4	2055.06494	2058	2.93506	0.05	0.475	0.75	0.090938298	0.106691484	0.119964628	0.058118031	0.05140592	0.047012899	0.005186665		
MONTNEY	2058	2074.5974	16.5974	4.05	8.375	11.025	0.174775309	0.202408168	0.219969501	0.065118811	0.08301278	0.05770261	0.045611411		
SB4	2074.5974	2090.18182	15.58442	4.675	9.65	12.95	0.195489574	0.212180087	0.218176767	0.067198065	0.06202721	0.057961848	0.049993584		
BSF3	2090.18182	2115.32468	25.14286	6.825	13.125	18.55	0.19009949	0.224811008	0.219524451	0.065408094	0.062243055	0.058917443	0.077702961		
MS3	2115.32468	2132.15584	16.83116	3.625	9.8	12.975	0.223486821	0.281637457	0.28007583	0.066104152	0.063055998	0.040681795	0.051279868		
TS3	2132.15584	2205.50649	73.35065	15.475	41.975	57.5	0.194093527	0.261170165	0.295082495	0.072864587	0.066535887	0.042117234	0.229559941		
SB3	2205.50649	2226.49351	20.98702	2.325	6.475	8.875	0.204856742	0.217879789	0.279515197	0.067057296	0.064270249	0.05910718	0.046464194		
BSF2	2226.49351	2252.47532	26.18181	0.325	2.75	8.575	0.173699736	0.43051546	0.467209186	0.118719051	0.064395047	0.05667496	0.040150458		
MS2	2252.47532	2262.85714	10.38182	0.925	4.025	6.35	0.257717274	0.319515931	0.347157326	0.05970618	0.066781426	0.043140611	0.027875054		
TS2	2262.85714	2269.50649	6.64935	0	1.3	3.9	0	0.345517104	0.370299156	0	0.067840375	0.057261919	0.016155472		
SB2	2269.50649	2356.36364	86.85715	0	8.6	21.85	0	0.421756829	0.484756306	0	0.076667848	0.068048873	0.128649848		
BSF1	2356.36364	2370	13.63636	0	3.975	8.1	0	0.415517346	0.4673961	0	0.084887146	0.075649177	0.015045289		
MS1	2370	2384.92408	14.92408	0	0.875	2.675	0	0.500640645	0.59178954	0	0.084849472	0.072933601	0.011989581		
SB1 BELLOY	2384.92408	2410	25.07592	0	0.6	1.85	0	0.543895133	0.304257564	0	0.07205296	0.047617758	0.010500048		



References

1. Eslinger, E., and R. V. Everett, 2012, 'Petrophysics in Gas Shales', in J. A. Breyer, ed., *Shale Reservoirs—Giant Resources for the 21st century: AAPG Memoir 97*, p. 419–451.
2. Eslinger, E., and Boyle, F., 'Building a Multi-Well Model for Partitioning Spectroscopy Log Elements into Minerals Using Core Mineralogy for Calibration', *SPWLA 54th Annual Logging Symposium*, June 22–26, 2013.
3. M. M. Herron, SPE, D. L. Johnson and L. M. Schwartz, Schlumberger-Doll Research, 'A Robust Permeability Estimator for Siliciclastics', SPE 49301, 1998 SPE Annual Technical Conference and Exhibition held in New Orleans, Louisiana, 27–30 September 1968.
4. Susan L. Herron and Michael M. Herron, 'Application of Nuclear Spectroscopy Logs To the Derivation of Formation Matrix Density' Paper JJ Presented at the 41st Annual Logging Symposium of the Society of Professional Well Log Analysts, June 4–7, 2000, Dallas, Texas.
5. Clavier, C., Coates, G., Dumanoir, J., 'Theoretical and Experimental Basis for the Dual-Water Model for interpretation of Shaly Sands', *SPE Journal Vol 24 #2*, April 1984.
6. Herron, M.M., 'Geochemical Classification of Terrigenous Sands and Shales from Core or Log Data', *Journal of Sedimentary Petrology*, Vol. 58, No. 5 September, 1988, p. 820–829.
7. Everett, R.V., Berhane, M, Euzen, T., Everett, J.R., Powers, M, 'Petrophysics Designed to Honour Core – Duvernay & Triassic' *Geoconvention Focus* May 2014.
8. Everett, R. V. 'CWLS Insite' Spring 2014.
9. Ghanbarian, B, Hunt, A. g., Ewing, R. P. Skinner, T. E., 'Universal Scaling of the Formation Factor in Porous Media Derived by Combining Percolation and Effective Medium Theories' *Geophysical Research letters*, 10.1002/2014GL060180, Ghanbarian-alavijeh.2@wright.edu
10. Herron, S. L., Herron, M. M., Pirie, Iain, Saldungaray, Craddock, Paul, Charsky, Alyssa, Polyakov, Marina, Shray, Frank, Li, Ting, 'Application and Quality Control of Core Data for the Development and Validation of Elemental Spectroscopy Log Interpretation', *SPWLA, 55th Annual Logging Symposium*, Abu Dhabi, United Arab Emirates, May 18–22, 2014.
11. Slatt R, internet http://www.searchanddiscovery.com/documents/2011/80181slatt/ndx_slatt.pdf <http://info.drillinginfo.com/seismic-brittleness-volume-estimation-from-well-logs-in-unconventional-reservoirs-part-iii/>
12. Euzen, Tristan, Everett, RV, Matthew Power, Vincent Crombez, Sébastien Rohais, Noga Vaisblat, François Baudin, 'Geological Controls on Reservoir Properties of the Montney Formation in Northeastern BC: An Integration of Sequence Stratigraphy, Organic Geochemistry, Quantitative Mineralogy and Petrophysical Analysis', *GeoConvention*, Calgary, May 2015.
13. Everett, RV, 'Three Methods for Log-Derived Mineralogy: Part Two ... Primarily Used for Shales (Silts) and Tight Formations and Also Applicable to High Porosity Formations' *InSite CWLS* April 2015.
14. Nieto, J, Bercha, R., Chan, J., 2009. *Shale Gas Petrophysics – Montney and Muskwa, are they Barnett Look-Alikes?* *SPWLA 50th Annual Logging Symposium*, June 21–24, 2009.
15. Michael M. Herron and Susan L. Herron, 'Real Time Petrophysical Evaluation System' Patent CA 2463058 A1, filed 23 Sept 2002.

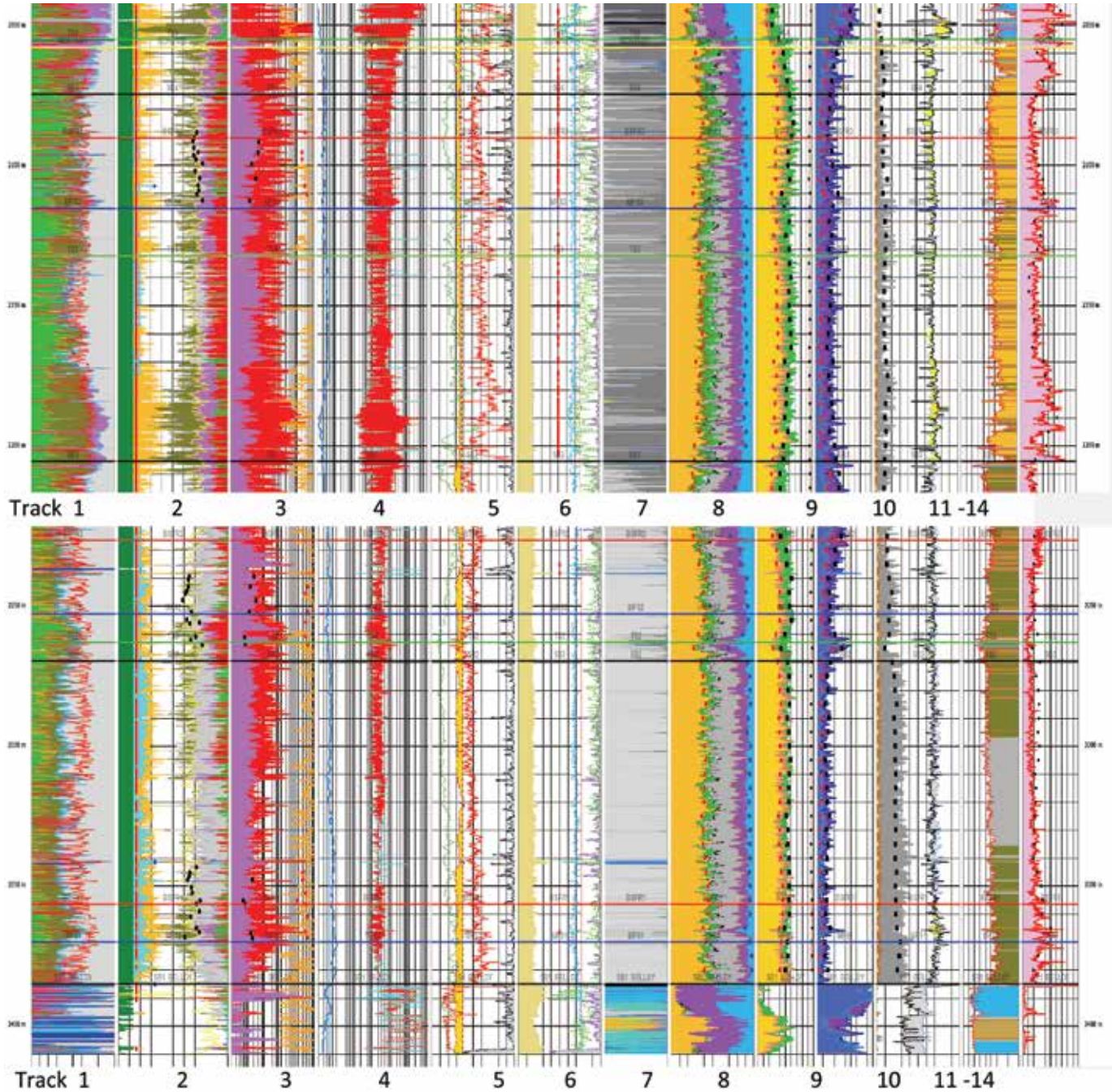


Figure A1-1A. 'Too Much Information plot'; look for trends.

Explanation of each track

Track 1: Water saturation, red is minimum Sw for water-free production (SW_DS_GAS_ECS)

Note that SW_DS_GAS_ECS is a curve developed in another well by Dean Stark Analysis. This other well did not have clay

so the SW_DS_GAS is a clay-free Sw. Consequently it will fall below the Swb curve in zones with high clay. Plot purple to right of SW_DS_GAS_ECS to Swt_R_ELM for immobile oil in the small capillaries. Green is oil to left of S_BFV (mobile oil); olive is immobile gas, kerogen and bitumen to right of S_BFV. The suffix _PRED means the BFV has limits applied



so the free fluid volume does not exceed effective porosity or go lower than zero porosity. The bound fluid volume is total porosity minus free fluid volume. There are two choices for the free fluid volume: 1) use CMFF which is derived from a T2_cutoff of 33 ms or 2) use CMRP_3MS which is derived from a 3ms cutoff. Tests in the lab indicated cutoff should be about 4.64 ms (5.68, 6.12 & 2.87). Since we cannot recalculate to incorporate the 4.64 ms, we chose the 3 ms as being more appropriate than 33 ms. When the free fluid volumes from 3 ms and 33 ms are plotted they are very close so the difference between 4.64 ms and 3 ms is the width of the curve line.

Track 2: Porosity with increases in plum-coloured HCPV in pay zones

Net pay is the green bar (porosity > 6% and hydrocarbon with no expected water production). The left of track 2 has a green area which is a cutoff for BVW. When Swt > green area, it indicates water could be produced. However, the orange curve gives the bound fluid volume, so when the blue BVW < BFV, no water will be produced even though it exceeded the cutoff. This situation happens when the bound water is large. In this well, no water will be produced.

Track 3: Perm with ECS perm in red, R_ELM perm in green; KSDR_CMV*0.1 perm in purple and KTIM*10 perm in orange.

The multipliers on KSDR and Timur were used to match the pulse decay perm at the low end and the RCA K_MAX perm at the high end. The reservoir perm is most likely in line with the pulse decay perm.

Track 4: Resistivity shows pay zones with red coding between the Ro and Rt

Track 5: SP, GR(s), uranium, and calipers

When the caliper is less than bit size, the difference is coded yellow.

Track 6: Neutron, density Pe, HDRA density correction

The neutron is neutron on a limestone matrix. Similarly, the density is a recorded density. If there is crossover on the matrix-adjusted density and neutron, the gas flag will turn on unless the density matrix-adjusted porosity is less than zero.

Track 7: Clustered lithology from merged runs, density, neutron, GR, and Pe

Track 8: Mineralogy from cuttings log QemScan

Track 9: Mineralogy derived from the robust element-to-mineral (R_ELM) in the master program, Geological Analysis by Maximum Likelihood Systems (GAMLS) (Ref. 1 and 2)

Track 10: Quartz, feldspar and muscovite (QFM) from the R_ELM program

The amount of muscovite, shown increasing to the left, from the right side of the track, is 0-6%, so is quite small. The match of logs and core is quite good. However, the difference in CEC content for illite plus muscovite and just illite is small, so the effect of not including the muscovite in the CEC on Sw will also be small.

Track 11: Carbonate track showing calcite and dolomite

The amount of other carbonates is small (siderite, apatite). Logs and core show a close match.

Track 12: Clay, primarily illite

The log illite is higher than the core illite but close. Also in this track is brittleness derived from the dipole sonic and also from the ratio of (dolomite + quartz) / (calcite + dolomite + quartz + clay + TOC), with all units in weight fractions. According to Dr. Roger Slatt (Ref. 11), the entire interval is 'High Brittle'.

Track 13: Sand Classification, modified from Herron (Ref. 6) by Mike Berhane (mike.berhane@aer.ca)

Note the Sand Class change at sequence boundary 3 (SB3). This change is also obvious on the cluster in Track 7, where the GR increases to a higher value above the sequence boundary. The higher GR is due to higher uranium, associated with the TOC, shown in the next Track 14.

Track 14: TOC from logs and core

Initially, uranium was used to calculate the TOC. It was then modified by a cluster with the TOC measurements from the cuttings.

The next plot shows how Swirr from the Coates-Timur equation separated the net pay from the net sand.

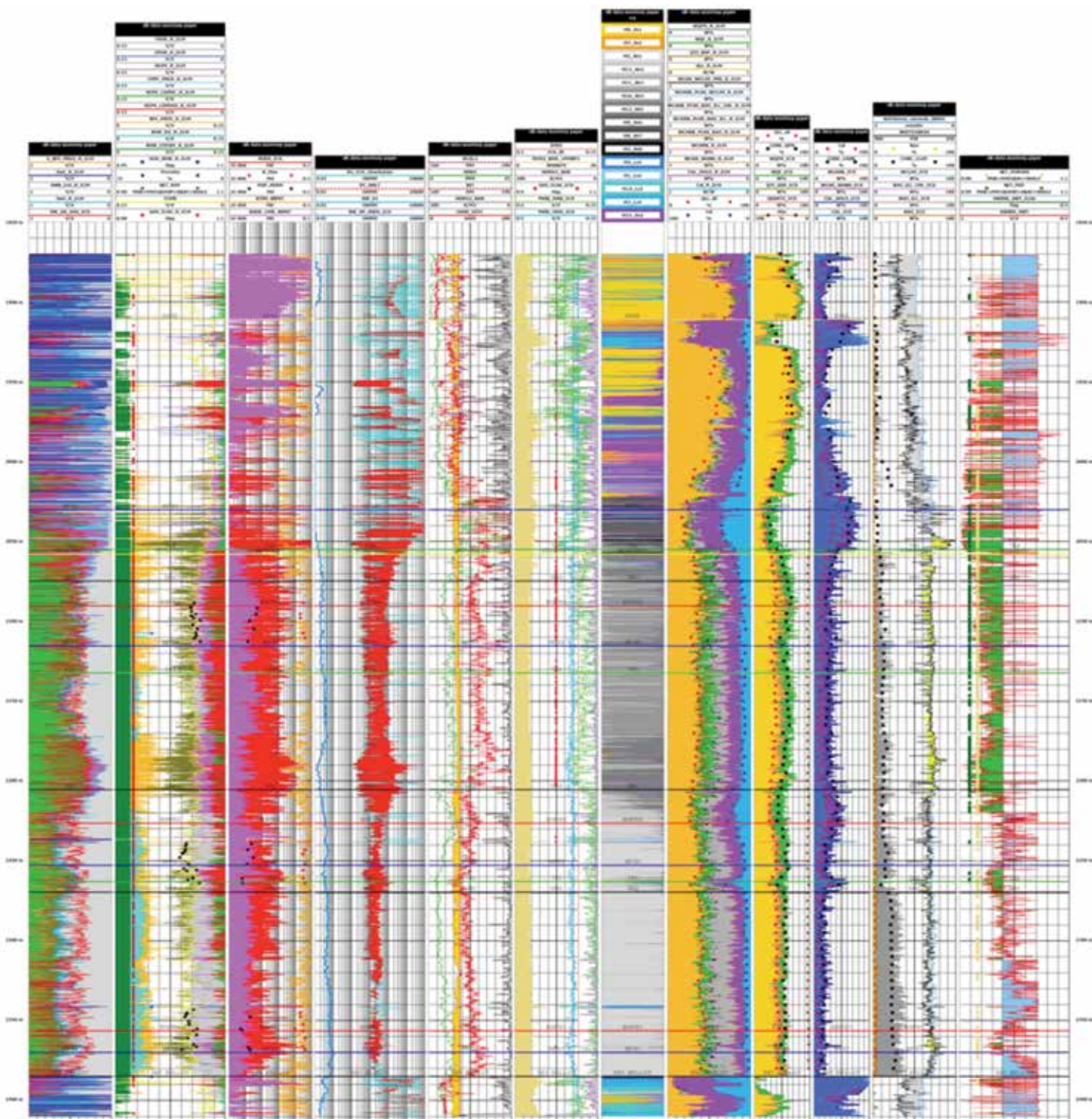


Figure A1-1B. Swirr separates pay: Track 12 shows Swirr to left of flag, for net pay.

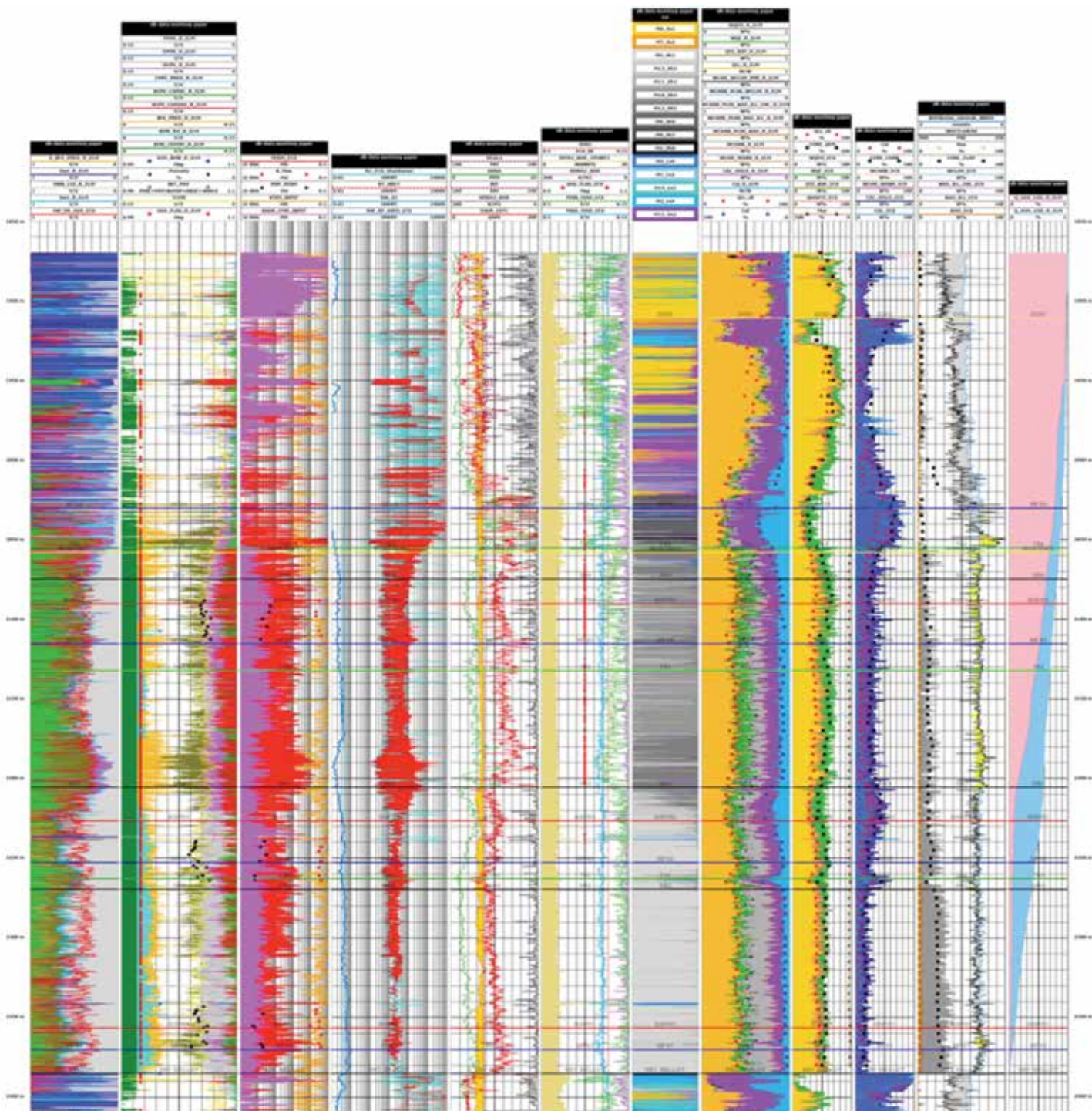


Figure A1-1C. Flow profile of Sw: actual flow will not occur due to the indication from BFV. The gas/oil starts to increase at SB3, whereas Sw is relatively constant above SB3. Look for slope changes.



Appendix B: Parameter criteria used

Pressure gradient 0.52 psi/ft; $T=0.0198 \cdot \text{ft} + 42 \text{ degF}$

TOPS & SUMMARY	WELL:	CSPG CWLS MAY 2015 P DATE:	2015-02-01 14.46.18
STRT:	1870 STOP:	2410	
PAY INPUT PARAMETERS			
IP_INPUT_PARAM_Flag		2 use old SWIRR (insert 1) or new SWI (insert 2) from Heron 2002 paper [Allowed: 1,2] [Excel: SC\$101] [Group: Pay]	
IP_INPUT_PARAM_C/W/W		40 maximum clay cutoff - eliminate net pay when clay is high. In some shale plays it will not apply so the value would be set to 100. [Allowed: 0-100] [Excel: SC\$102] [Group: Pay]	
IP_INPUT_PARAM_Flag	YES	Enable logic to use bulk volume of water in net pay determination [Allowed: yes,no] [Excel: SC\$103] [Group: Pay]	
IP_INPUT_PARAM_Flag	yes	Enable anhydrite gas flag impact check. With anhydrite, the neutron porosity (PHIN_MAN) is less than the density porosity (PHID_MAD) thus incorrectly turning the gas flag on. Anhydrite has zero porosity thus no possib...	
IP_INPUT_PARAM_C/V/V		0.03 Pseudo resistivity porosity threshold [Allowed: 0.001-100] [Excel: SC\$105] [Group: Pay]	
IP_INPUT_PARAM_GROUP/SC\$106		0.3 A pseudo resistivity that ensures pay calculated from the Archie formula $Rt_{Pay} = FRW / Swt^n \cdot Tpor \cdot mRw / Sw^n$ [Allowed: 0.001-100] [Excel: SC\$106] [Group: Pay]	
IP_INPUT_PARAM_Flag	no	Enable logic to use pseudo resistivity (Rt_Pay) in net pay determination [Allowed: yes,no] [Excel: SC\$107] [Group: Pay]	
IP_INPUT_PARAM_C/V/V		1.2 BVW cutoff multiplier (Montney=2.66, Duvernay=4.1, Muskwa=4.5, Sudan conv gas=3.5, Sudan conv oil=5.3) [Allowed: 0.1-20] [Excel: SC\$2] [Group: Pay]	
IP_INPUT_PARAM_C/V/V		0.04 Pay1 PHIE=06 (includes CMFF_HC>0.03 and K=0.001 and OOIP>0 and sandclass=SHALE(0.5)) and Sw-Sw_crit=0.4 and perm_TT wells=0.001 and SWIRR=>Swt [Allowed: 0-1] [Excel: SC\$48] [Group: Pay]	
IP_INPUT_PARAM_C/V/V		0.04 Pay2 PHIE=06 (and sandclass=shale(0.5)) [Allowed: 0-1] [Excel: SC\$49] [Group: Pay]	
IP_INPUT_PARAM_C/V/V		0.03 Pay3 PHIE=03 (and sandclass=shale(0.5)) [Allowed: 0-1] [Excel: SC\$50] [Group: Pay]	
IP_INPUT_PARAM_GROUP/SC\$55		0.6 exponent in VIRR equation (Tpor / (FERM * VIRR_EXP) / (10 * (TPOR * 0.5))) + 1, default is 0.25) [Allowed: 0.0-1] [Excel: SC\$55] [Group: Pay]	
IP_INPUT_PARAM_GROUP/SC\$56		0 VIRR addition factor (usually zero) [Allowed: 0-1] [Excel: SC\$56] [Group: Pay]	
IP_INPUT_PARAM_C/V/V		0.4 Swt_ecs minus SWCRIT_hld difference for net pay flag to turn on [Allowed: -1.0 : 1.0] [Excel: SC\$86] [Group: Pay]	
IP_INPUT_PARAM_CM		0.001 minimum perm Perm_ECS for net pay [Allowed: 0.0000001-100] [Excel: SC\$87] [Group: Pay]	
IP_INPUT_PARAM_C/V/V		0 MINIMUM HCPV-CAPHC (FREE HC) FOR NET PAY [Allowed: 0-1] [Excel: SC\$88] [Group: Pay]	
IP_INPUT_PARAM_ratio		0.45 minimum sand class for NET PAY (Shale is 0.5) for log(SIO2/AL2O3) [Allowed: 0-2.5] [Excel: SC\$89] [Group: Pay]	
IP_INPUT_PARAM_ratio		0.45 minimum sand class for NET POROUS (Shale is 0.5) for log(SIO2/AL2O3) [Allowed: 0-2.5] [Excel: SC\$90] [Group: Pay]	
IP_INPUT_PARAM_ratio		0.45 minimum sand class for GROSS POROUS (Shale is 0.5) for log(SIO2/AL2O3) [Allowed: 0-2.5] [Excel: SC\$91] [Group: Pay]	
IP_INPUT_PARAM_MMBO/SECT		0 Minimum of OOIP for net pay [Allowed: 0-100] [Excel: SC\$92] [Group: Pay]	
IP_INPUT_PARAM_CM		10000 If Perfs=1, Net Pay =1, top depth [Allowed: 0-100000] [Excel: SC\$93] [Group: Pay]	
IP_INPUT_PARAM_CM		10000 If Perfs=1, Net Pay =1, btm depth [Allowed: 0-100000] [Excel: SC\$94] [Group: Pay]	
IP_INPUT_PARAM_Flag	yes	use log((SIO2+CaO)/AL2O3) instead of log(SIO2/AL2O3)? [Allowed: yes, no] [Excel: SC\$95] [Group: Pay]	
IP_INPUT_PARAM_Flag	no	Enable logic to turn off net pay below oil-water contact [Allowed: yes, no] [Excel: SC\$97] [Group: Pay]	
IP_INPUT_PARAM_C/V/V		0.45 Iriducible (Coates-Timur) minus total water saturation for net pay flag to turn on [Allowed: 0-1] [Excel: SC\$98] [Group: Pay]	

The selected output LAS curves. Executive Summary: the bare bones results that a geophysicist, reservoir engineer or geologist might want to use is called the WELL_NAME_ECS_SUMMARY.las.

Appendix C: Correction of density log

(Everett-modified after Poupon method)

Normal steps:

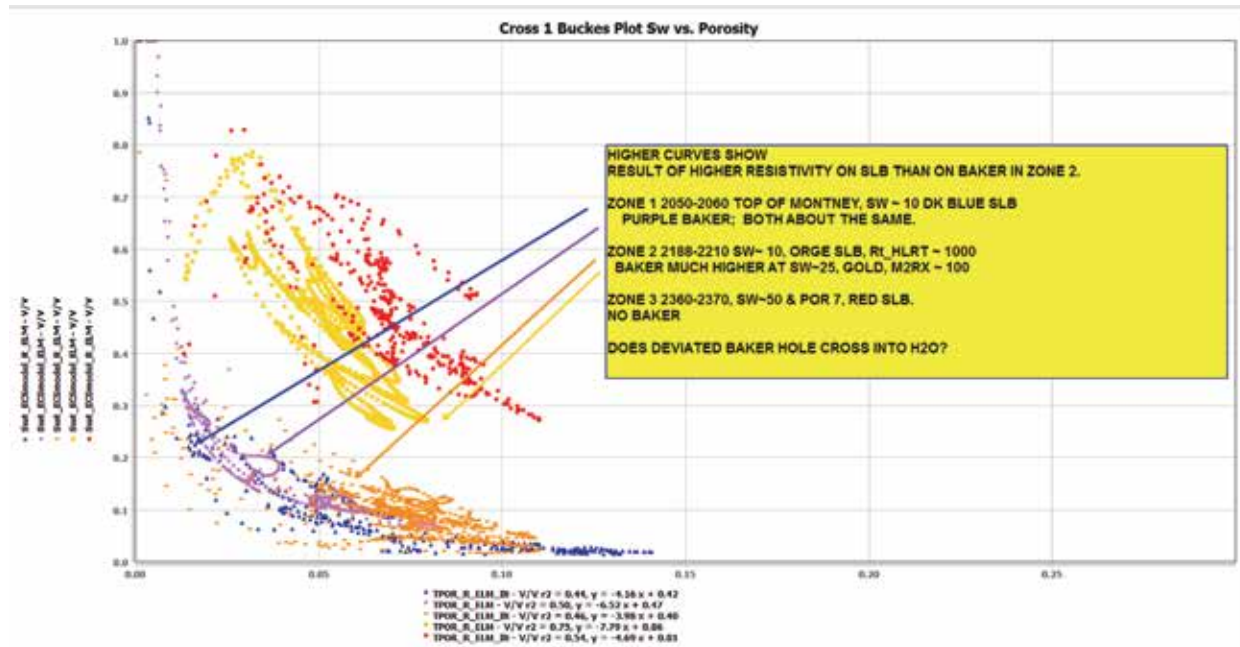
1. Look at Raw data high density correction (DRHO, HDRA etc.) near interesting zones. Display density log and DRHO which shows when pad does not make contact with the wall of the hole. Values below 2 g/c3 (middle of track) are suspect.
2. Display density and sonic porosity to identify where density porosity (LS) > sonic porosity (LS) as this should never happen unless the washout (check calipers and HDRA) make the apparent density porosity too high.
3. Check shading where sonic porosity is greater than density porosity; several iterations were made.
4. Compare corrected density to original density and use original density when it is greater (more dense) than corrected density. Label output as RHOB_CORR.



Appendix D: Mineral Models & Sw vs. porosity plots

Sw vs. Porosity

Below is a 'Buckles Plot'. The minimum BVW irreducible could be lower than that used for the bottom. The main point of this plot is that no water is expected to be produced above SB3.



The plot illustrates that the BH M2Rx reads lower than the SLB Rt_HLRT in Zone 2 from 2188-2210. In Zone 1, 2050-2060 both BH and SLB read the same. So we do not have a tool problem, we have a formation problem: the deviated BH hole may have crossed into a shaly water zone similar to the deeper red Zone 3 (logged by SLB but not reached by BH).

Mineral model

The minerals are derived from using the elements of the lithoScanner log. Below is the 'ECS-computer-model' result:

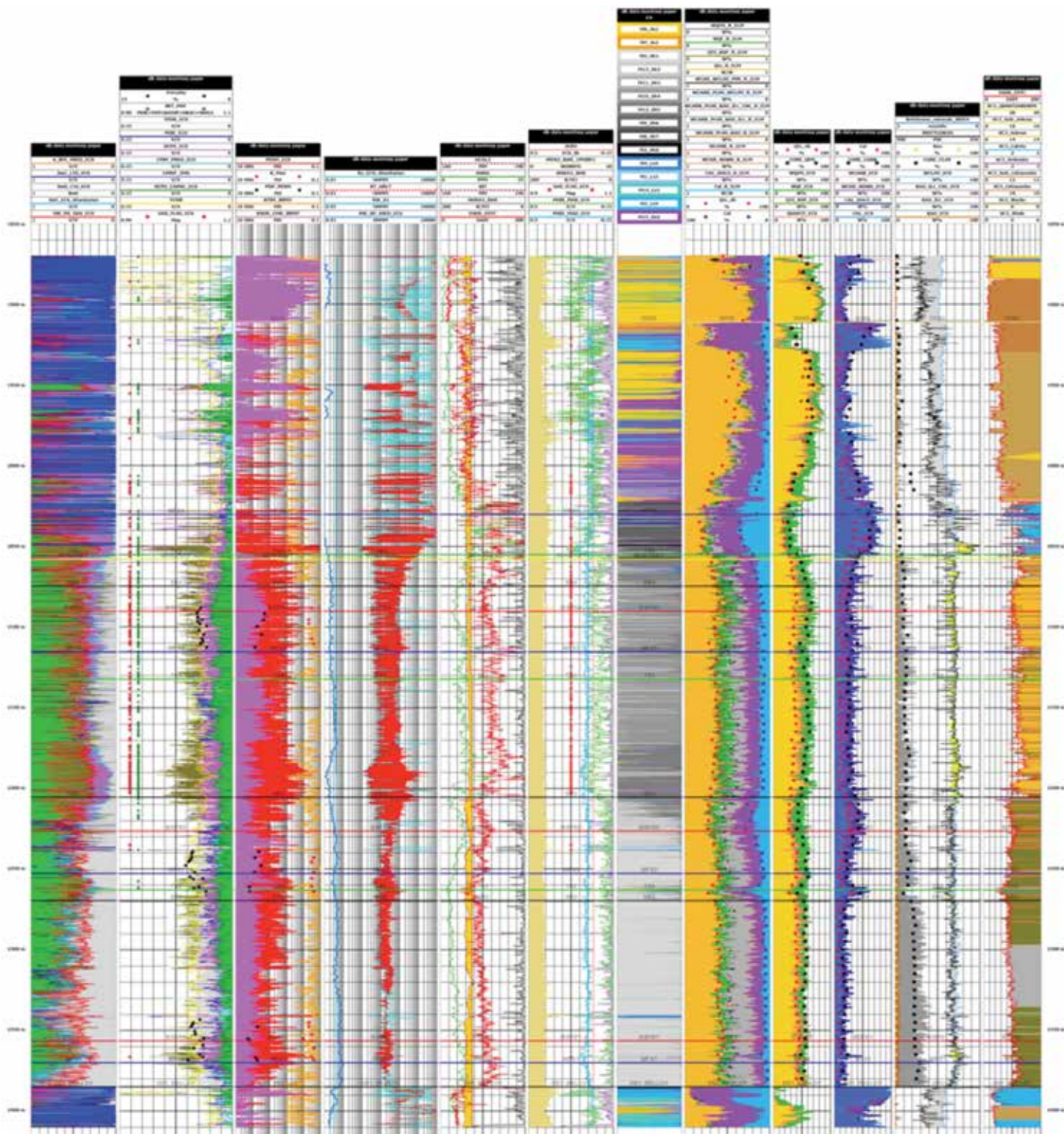


Figure D-1. Minerals from ECS calculation. They are very close to the R_ELM calculation.



Below are the Sw, Por, perm from BH minerals from the deviated hole, using the BH Flex elements, to derive minerals:

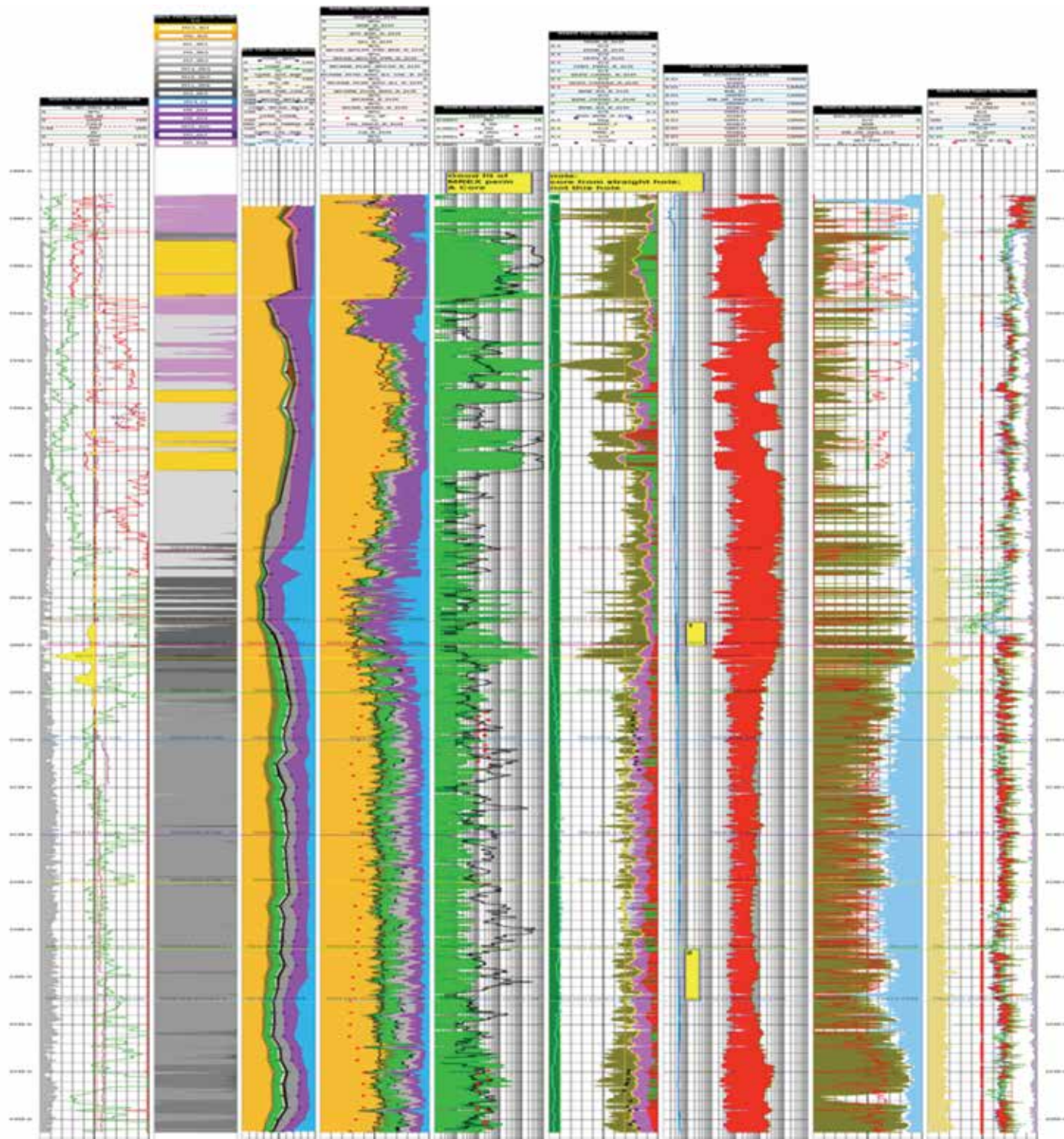


Figure D-2. Minerals from R_ELM calculation of the BH Flex data.

The elements Al, Ca, Fe, Si, S, and K are input to the PDHC (output is labeled as 'xxx_ECS') and Robust Elm (output is labeled as 'xxx_R_ELM') programs to output mineralogy, permeability, and grain density for porosity. In addition, calculate the S_w and porosity and validate outputs.

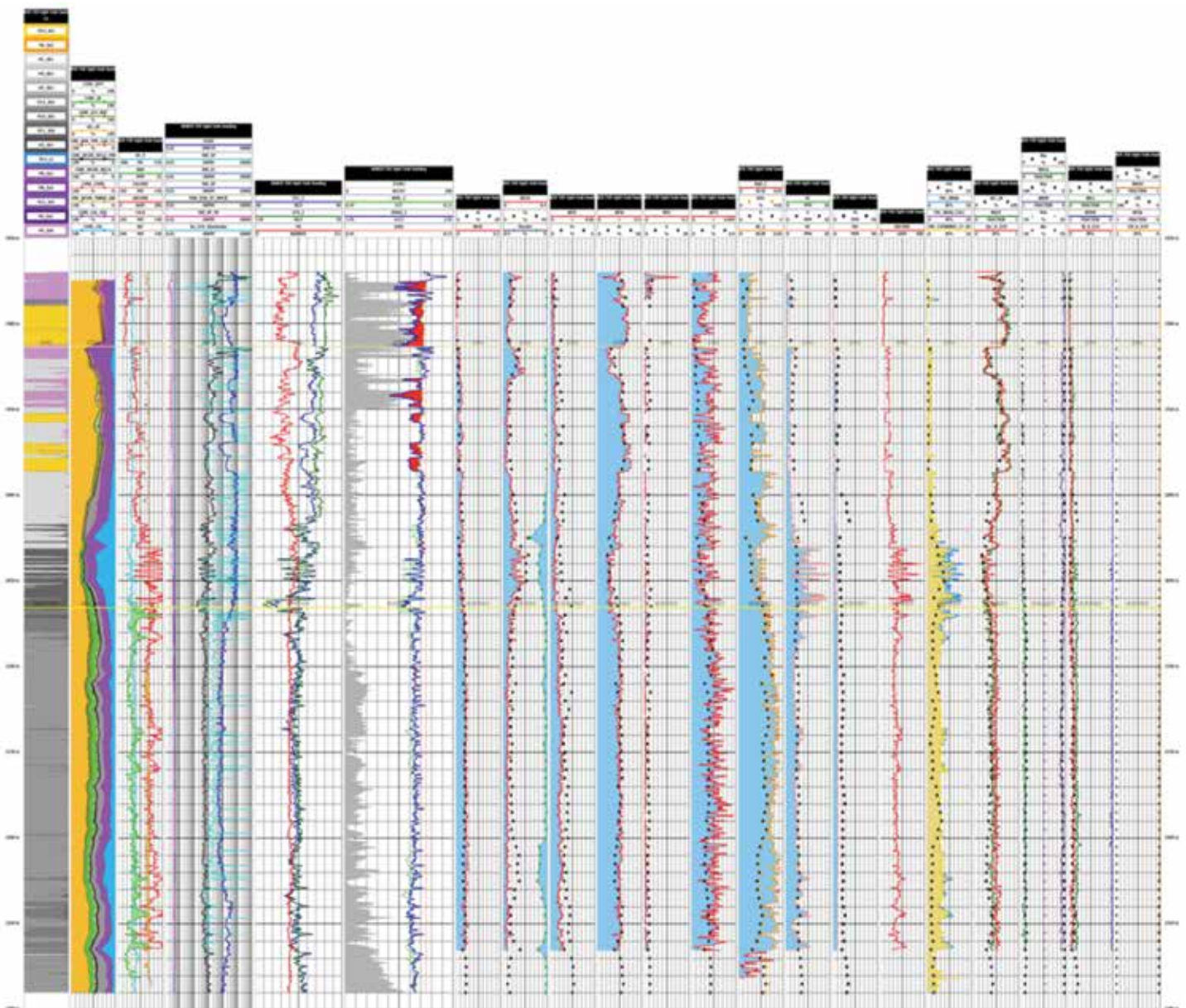


Figure D-3. Minerals from R_ELM calculation of the bh Flex data. Recall that the elements and minerals were from the straight hole, not from this deviated hole. Hence we don't expect them to fit perfectly.

Appendix E: Explanation of Sw coding

Step 1: Plot the Bound fluid volume for the R_ELM Track 1 and the ECS Track 2. Note that while the BFV is the same for both, the S_BFV is different because:

1. The BFV is TPOR-CMFF_PRED. Note that the BFV is normally calculated used TCMR-CMFF, not TPOR-CMFF_PRED. CMFF_PRED is CMRP_3MS limited to not exceed effective porosity. Since the vertical resolution of the density log and the CMR log may be different, this limit is imposed. For the R_ELM and the ECS calculations, effective porosity is different. Hence the S_BFV is different. Code the S_BFV as an orange curve and fill with green for movable oil from left track to S_BFV.

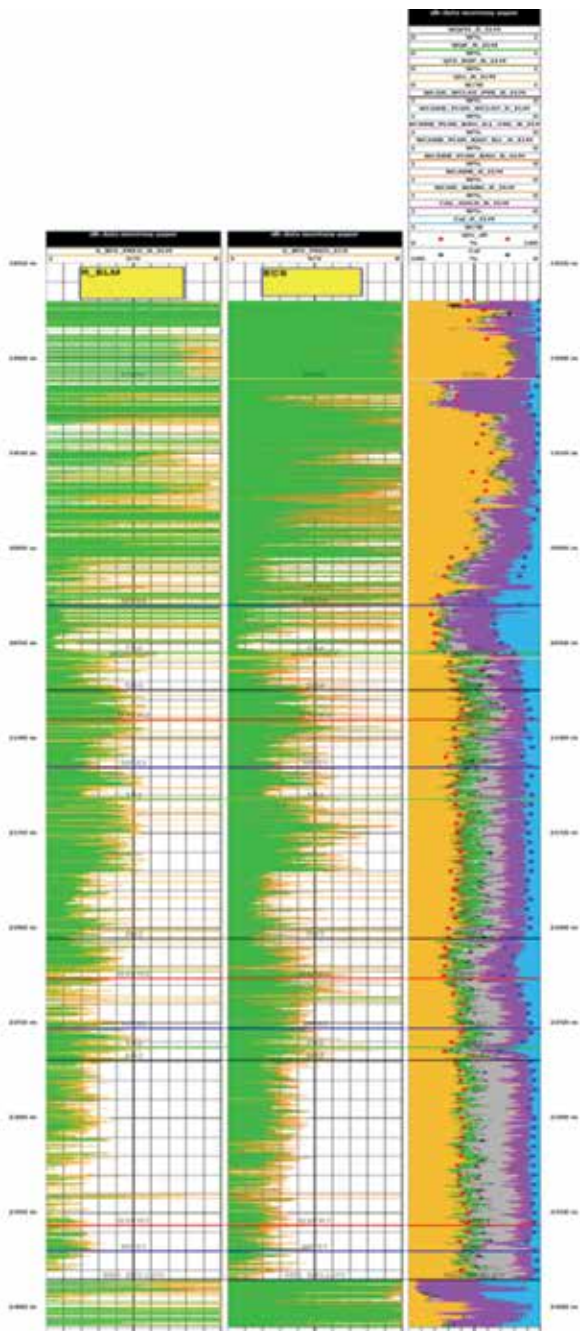


Figure E-2. Step 2: add Swt and code from Swt to right with Blue1 shading.

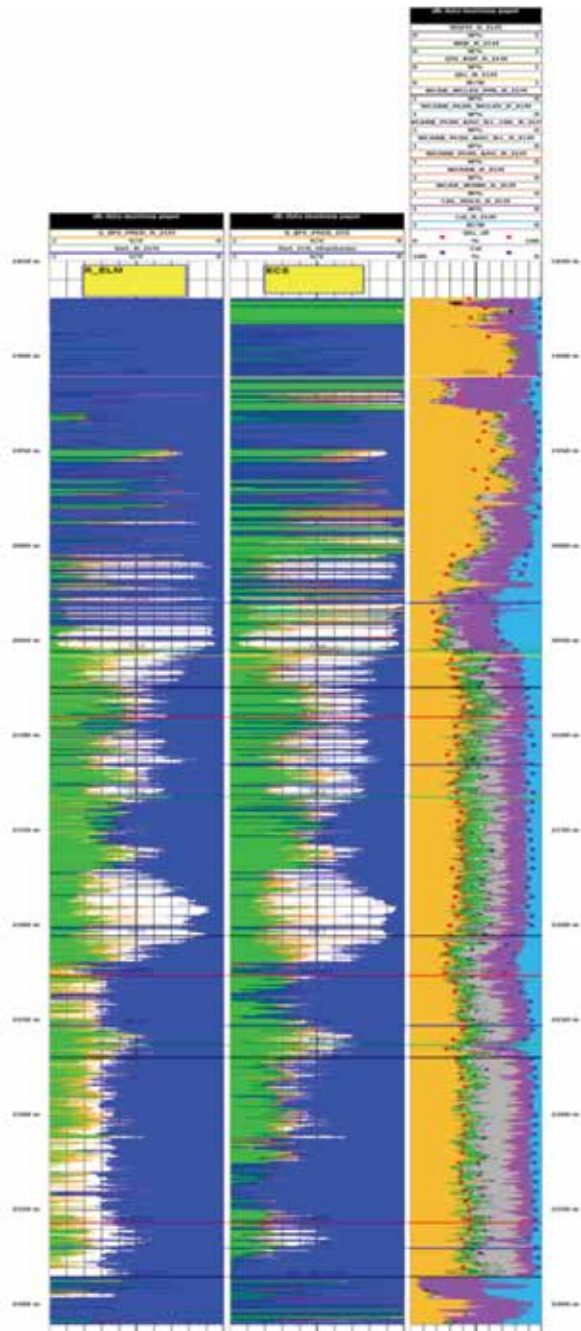


Figure E-2. Step 2: add Swt. The white space represents non-mobile fluids; note we are using the Ghanbarian model for formation Factor (Ref. 9).

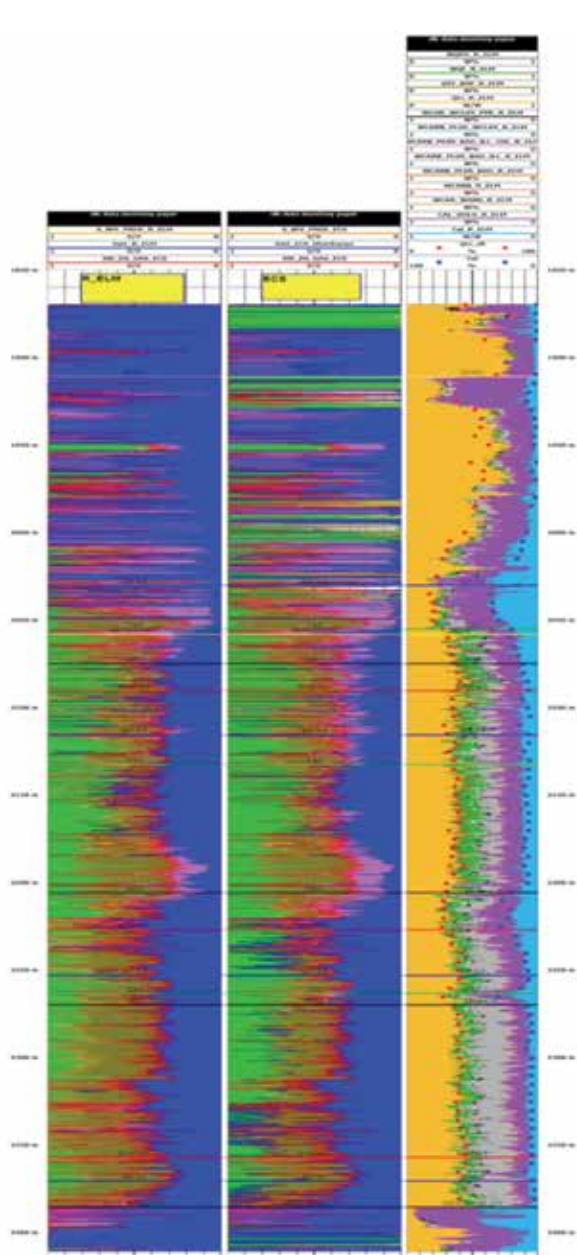


Figure E-3. Step 3 add SW_DS_GAS. This represents the non-shaly formation Sw-irreducible.

Figure E-3. Step 3 Add Sw_DS_Gas and code left to S_BFV as olive to represent the immovable kerogen, bitumen and 'unseen-by-the-NMR-gas'. Code to the right as a plum-purple, to represent hydrocarbon in the small capillaries. If there was no clay, we would be finished. However, due to the presence of clay discussed earlier, we add Swb.

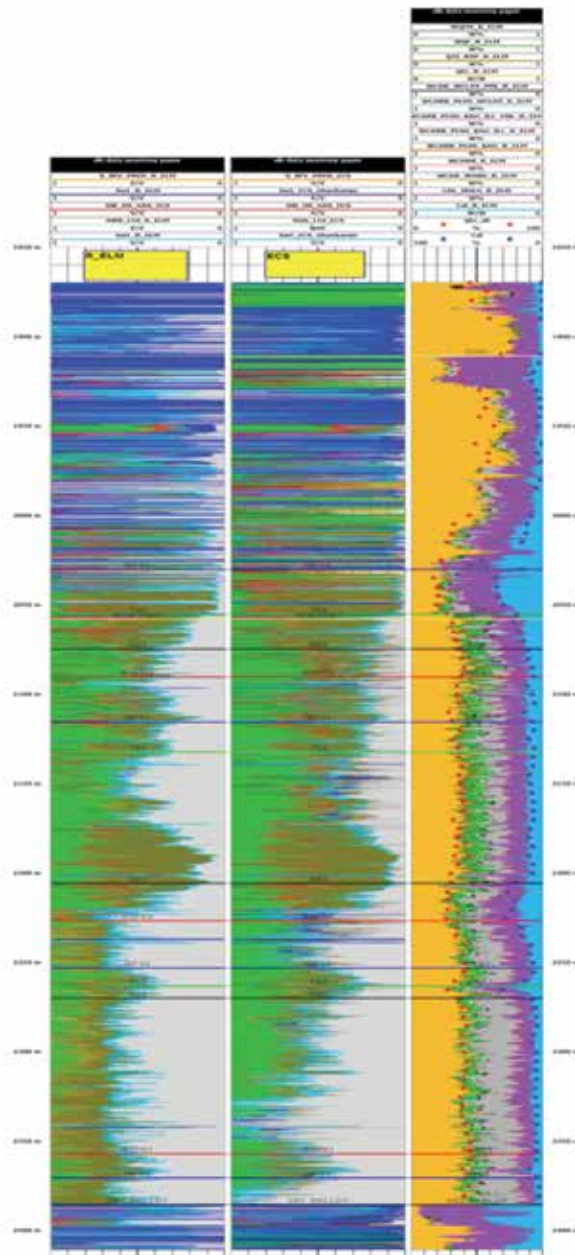
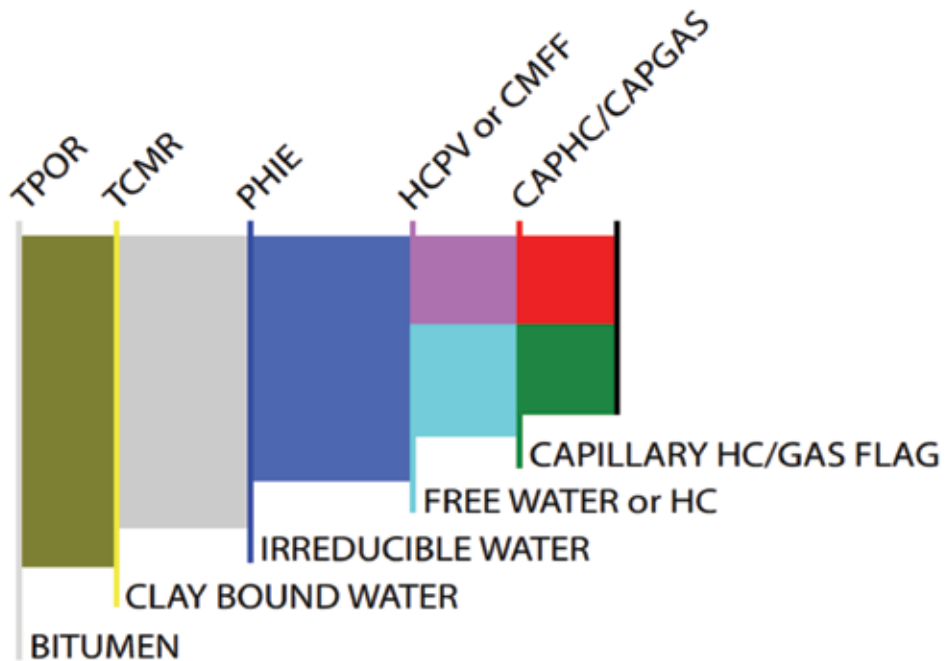


Figure E-4. Step 4, add Swb and code grey to the right track. Also add Swt to show that Swb is limited to Swt. Now complete, we can see there is no movable water as the clay water occupies what would have been mobile water. SW_DS_GAS can be added again but it has served its purpose already. However, we will add it to differentiate Swt below the Sw_DS_Gas with purple.



Appendix F: Explanation of Porosity coding

Image courtesy of Dr. Tristan Euzen.



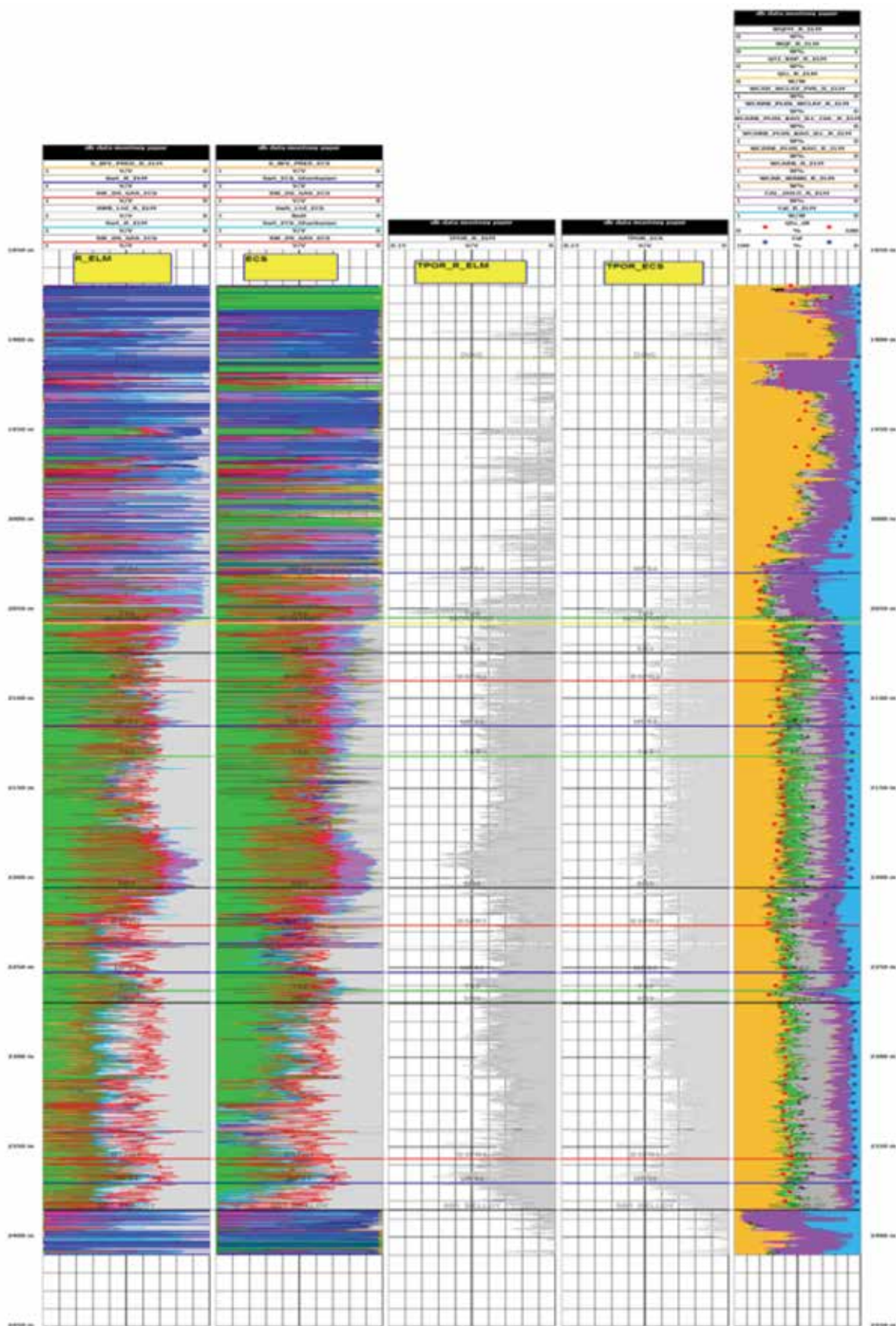


Figure F-1. Step 1: plot total porosity. Tracks 3 & 4, TPOR; SHADE GREY TO RIGHT to represent bound water.

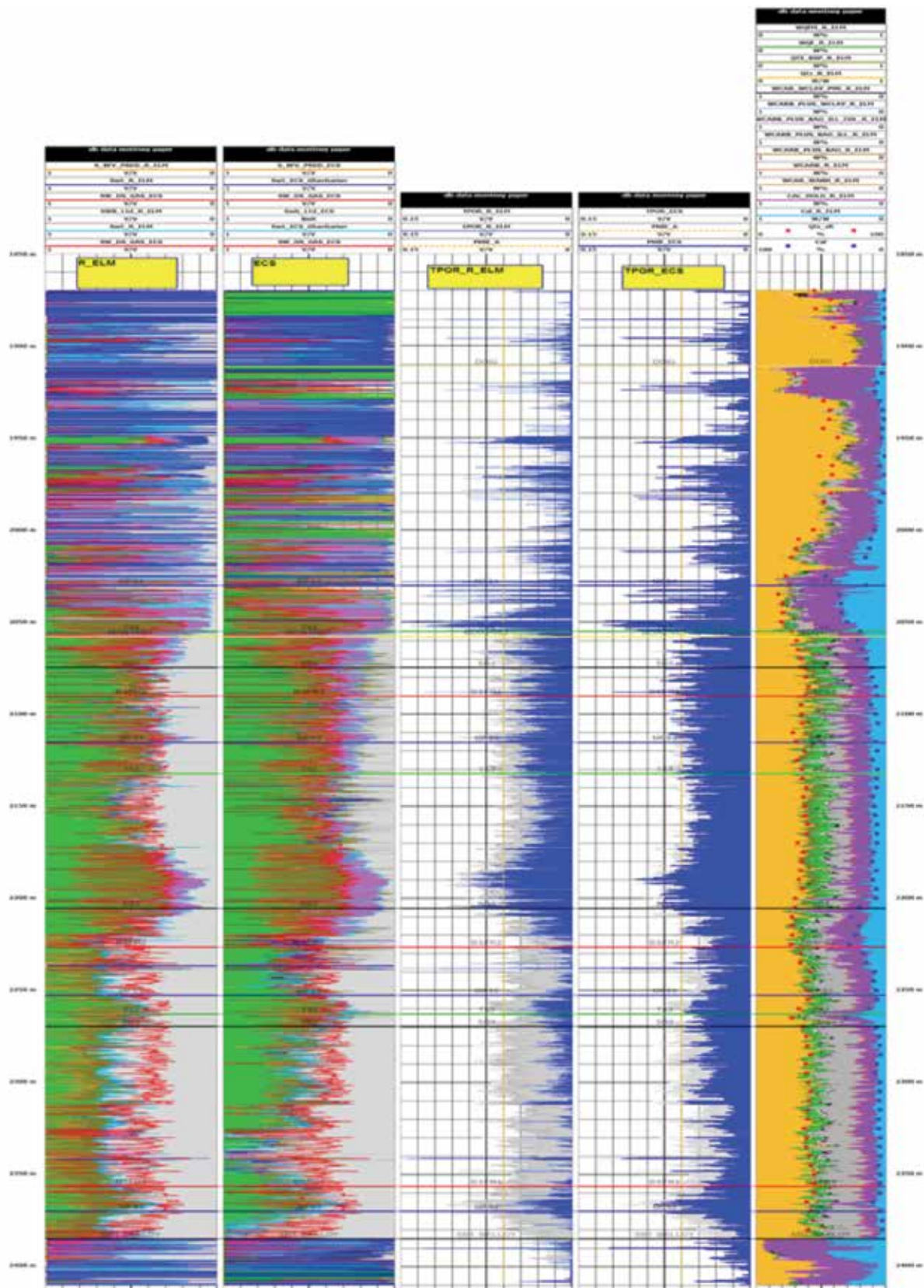


Figure F-2. Step 2: plot effective porosity, PHIE or EPOR, Tracks 3 & 4. Shade to right with blue to represent water trapped in capillaries.

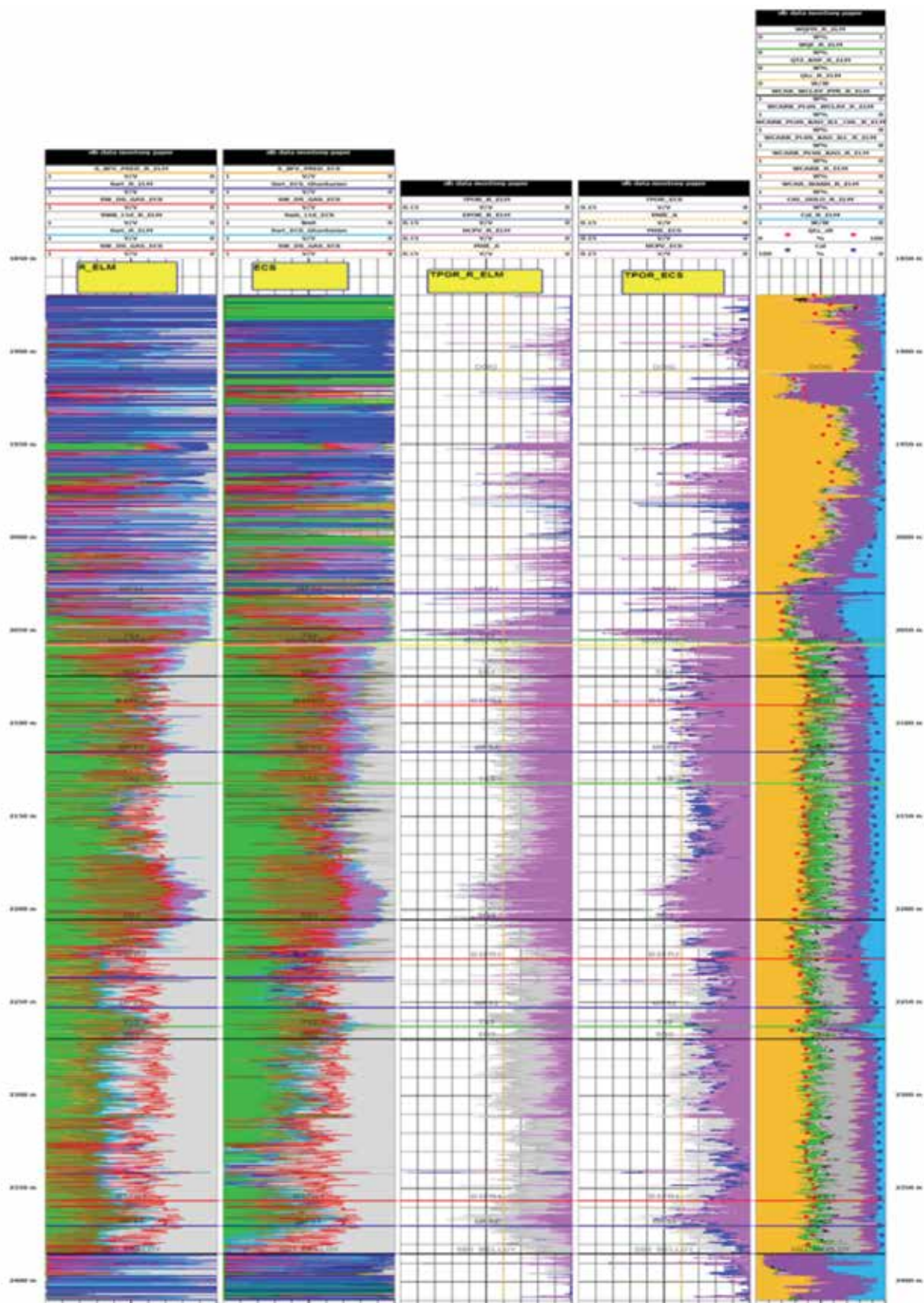


Figure F-3. Step 3: plot total porosity minus bulk volume of water, tracks 3 & 4, $TPOR - BVW = HCPV$. Shade plum to represent hydrocarbons trapped in the capillaries. For the moment, assume all HCPV is trapped.

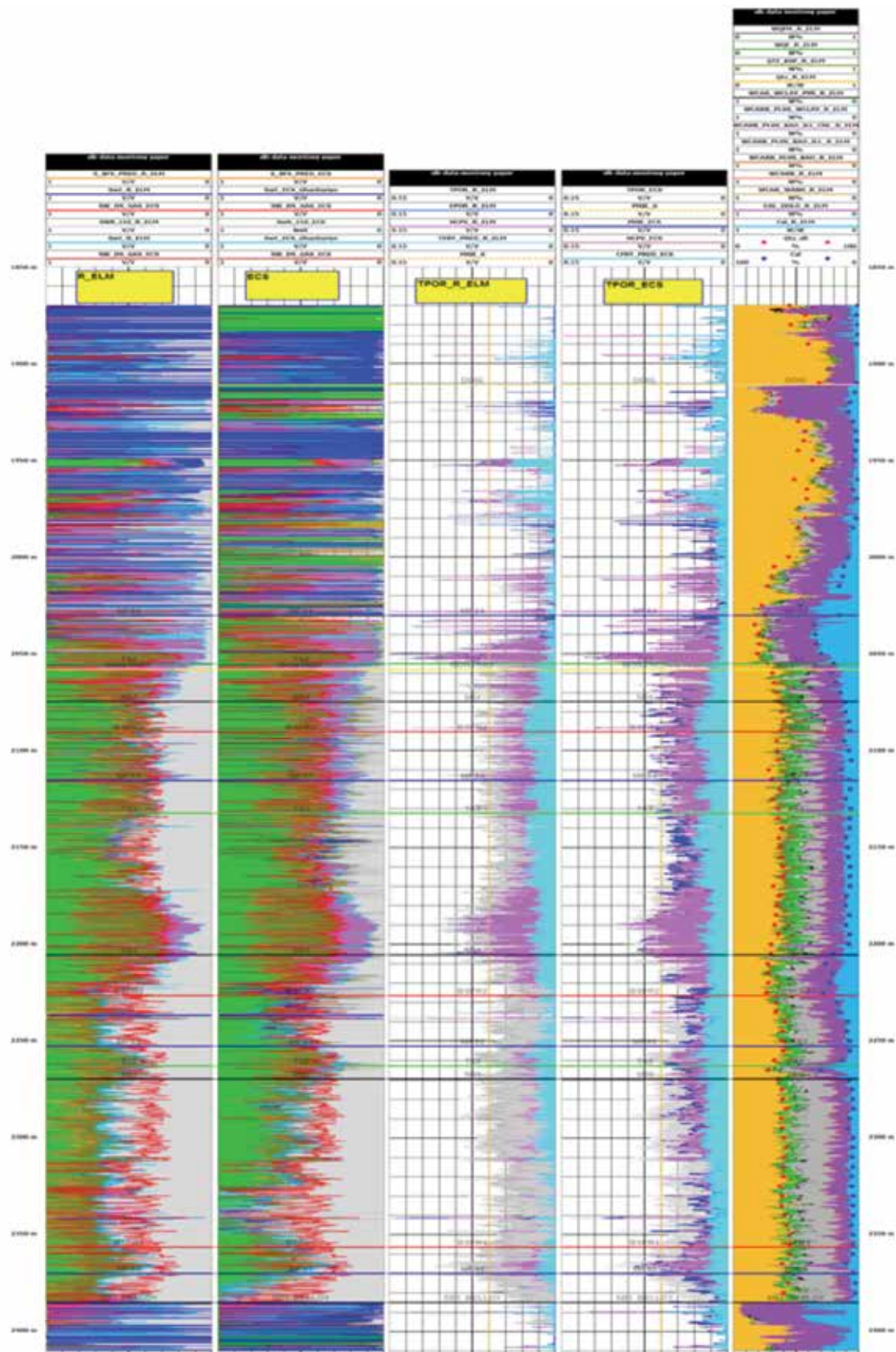


Figure F-4. Step 4: plot free porosity, Tracks 3 & 4, CMFF, and shade cyan as water in the free pore space. For the moment, assume all free porosity is water-filled.

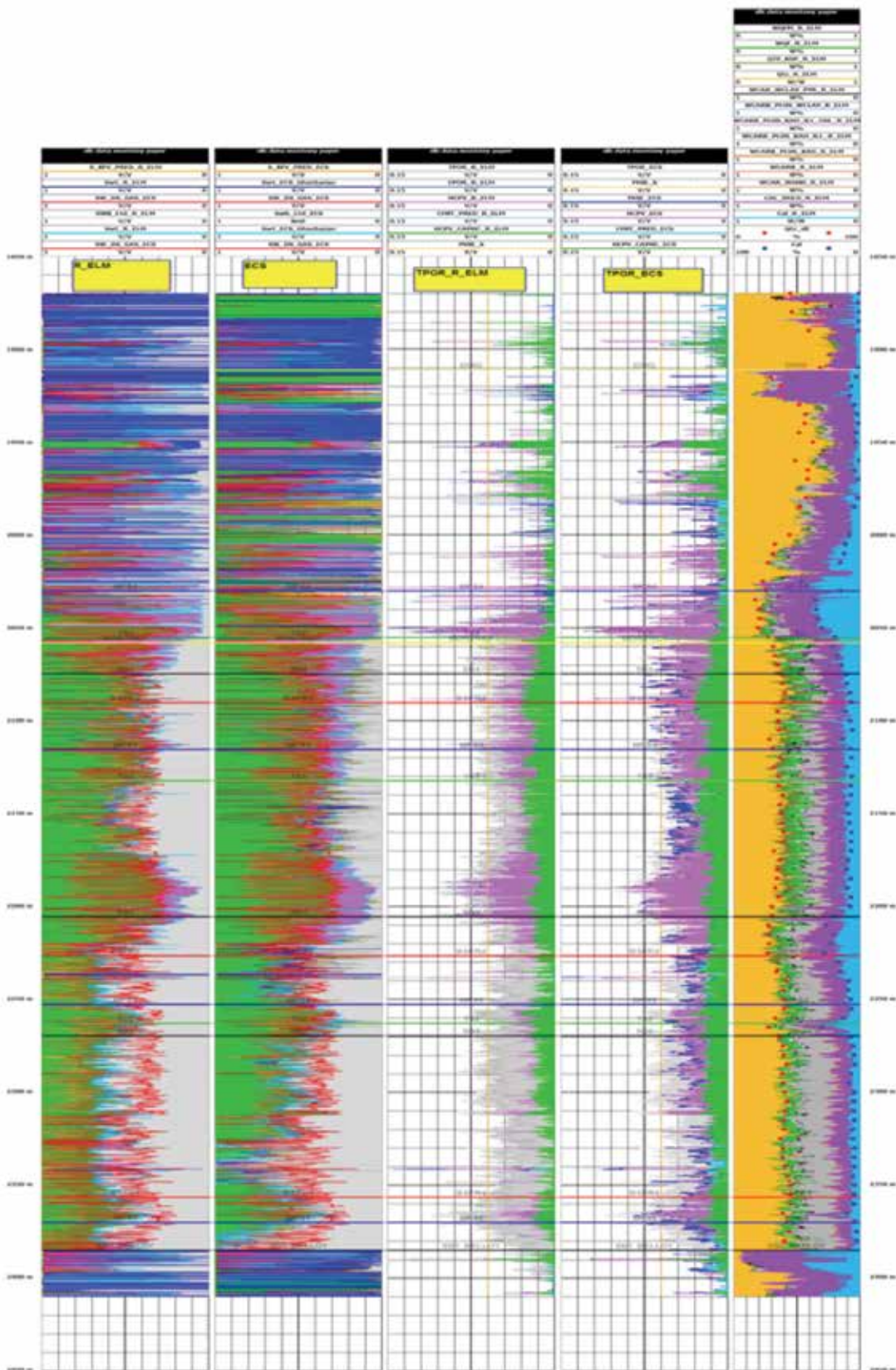


Figure F-5. Step 5, plot HCPV minus Capillary HC, tracks 3 & 4; Shade green oil to right to represent mobile oil in larger pores. Now we have made a distinction about what fluid is in the free pore space: oil or water.

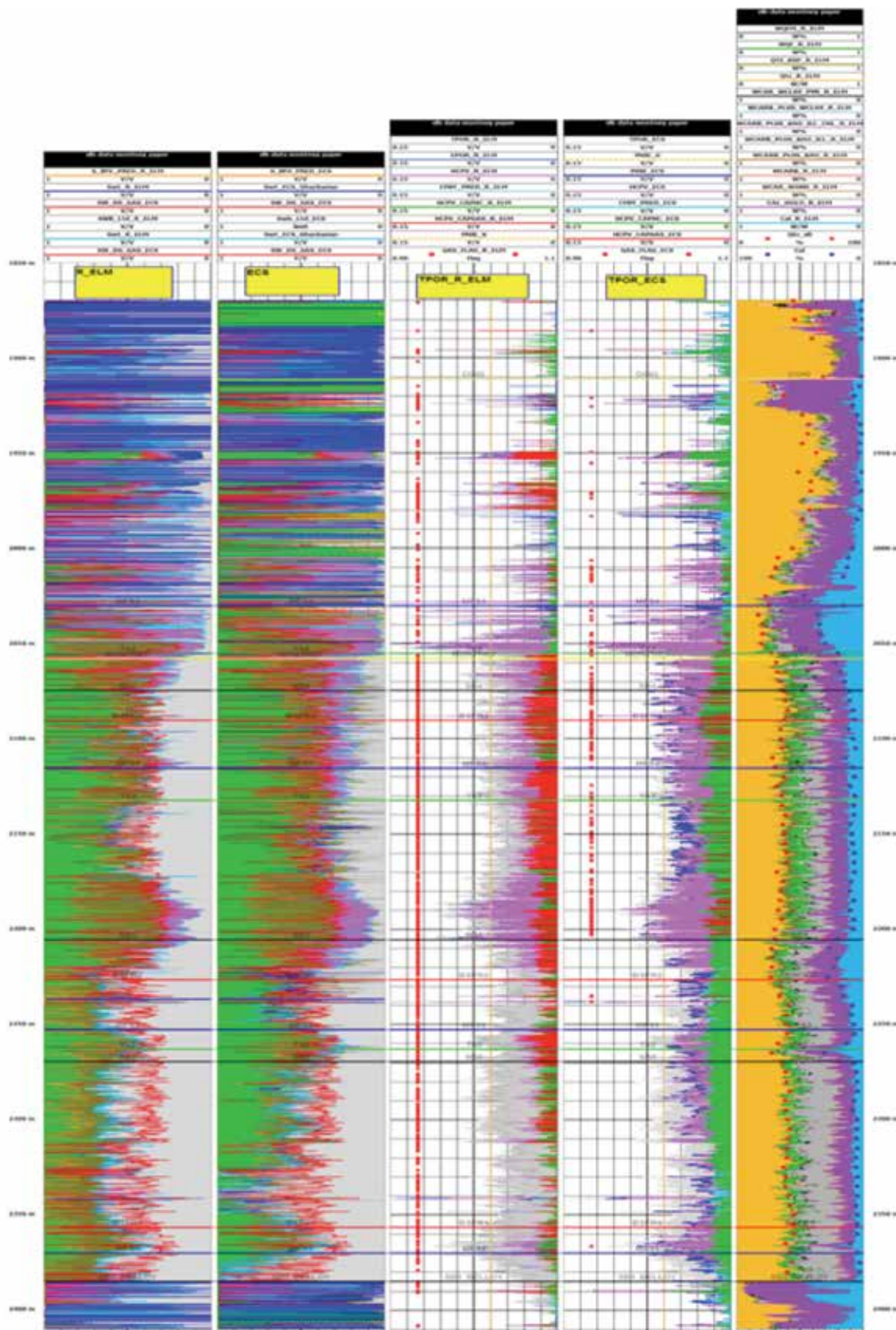


Figure F-6. Step 6, plot HCPV minus capillary gas. Note the gas flags are different when theoretically they should be the same. It is due to two different programs that they come out to be different. When the gas flag is on, then the HCPV_CAPHC is changed to HCPV_CAPGAS (shaded red). Hence, the ECS calculation says more oil than the R_ELM. The correct answer from offset production is more gas than oil.

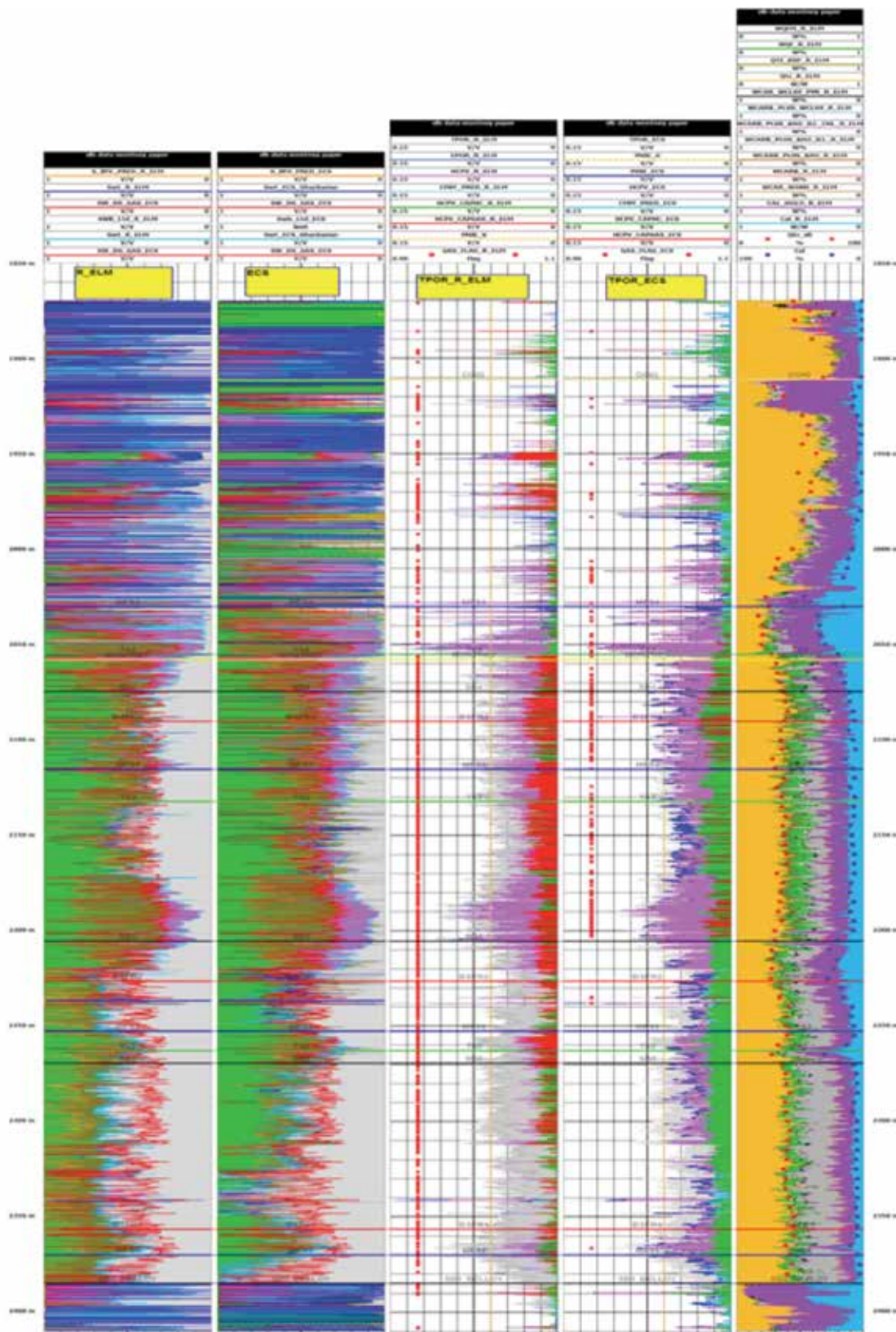


Figure F-7. Step 7; tracks 3 & 4, plot irreducible BVW from $SW_{DS_GAS} * TPOR * multiplier$, called BVW_CUTOFF. Shade green to left.

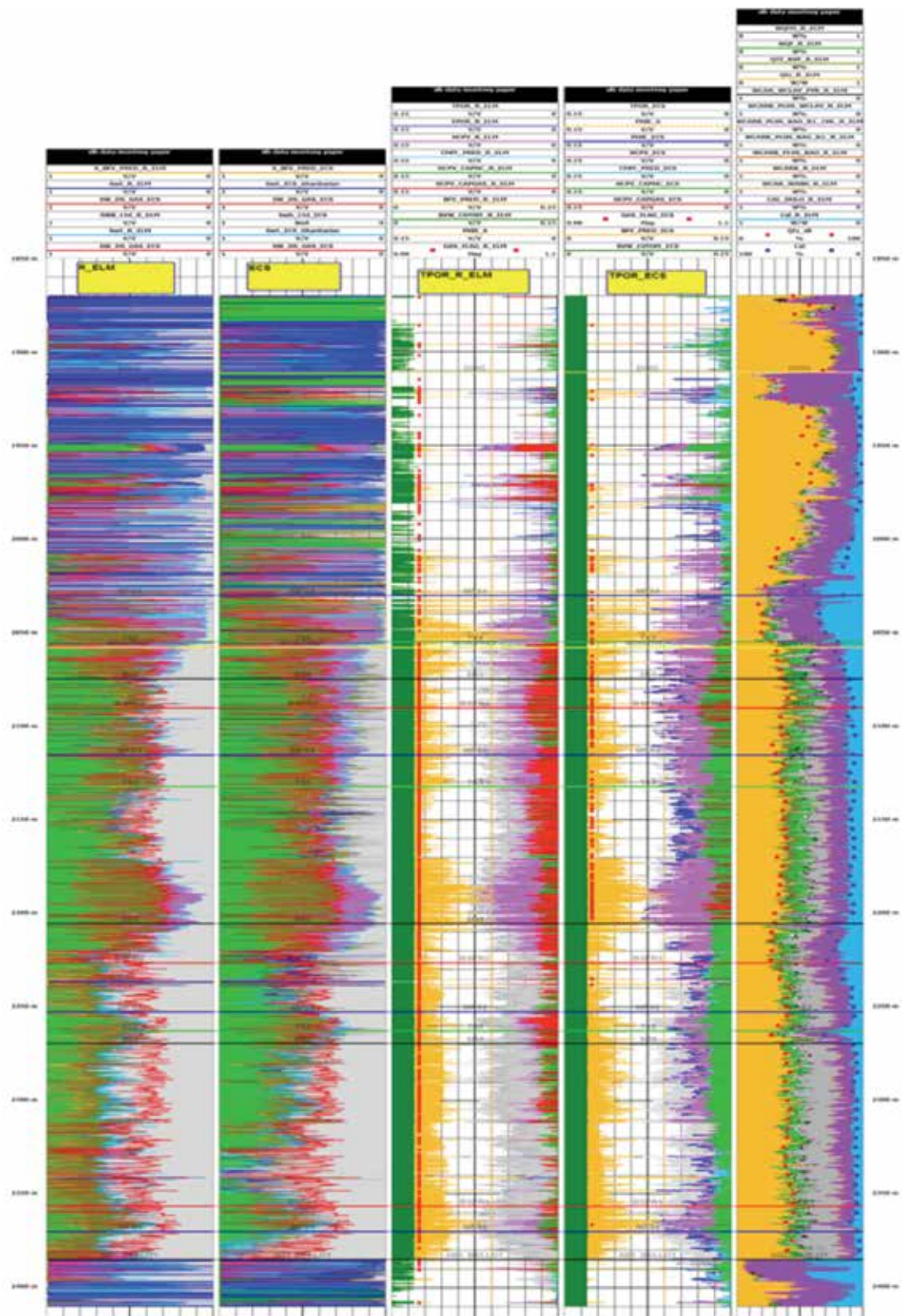


Figure F-8. Step 8: tracks 3 & 4, plot BFV (bound fluid volume from NMR) and shade orange to the left. The BVW must be less than BFV for no water to be produced, which is the case for this well. In the next figure, the BVW is plotted on top of the BFV so it can be seen.

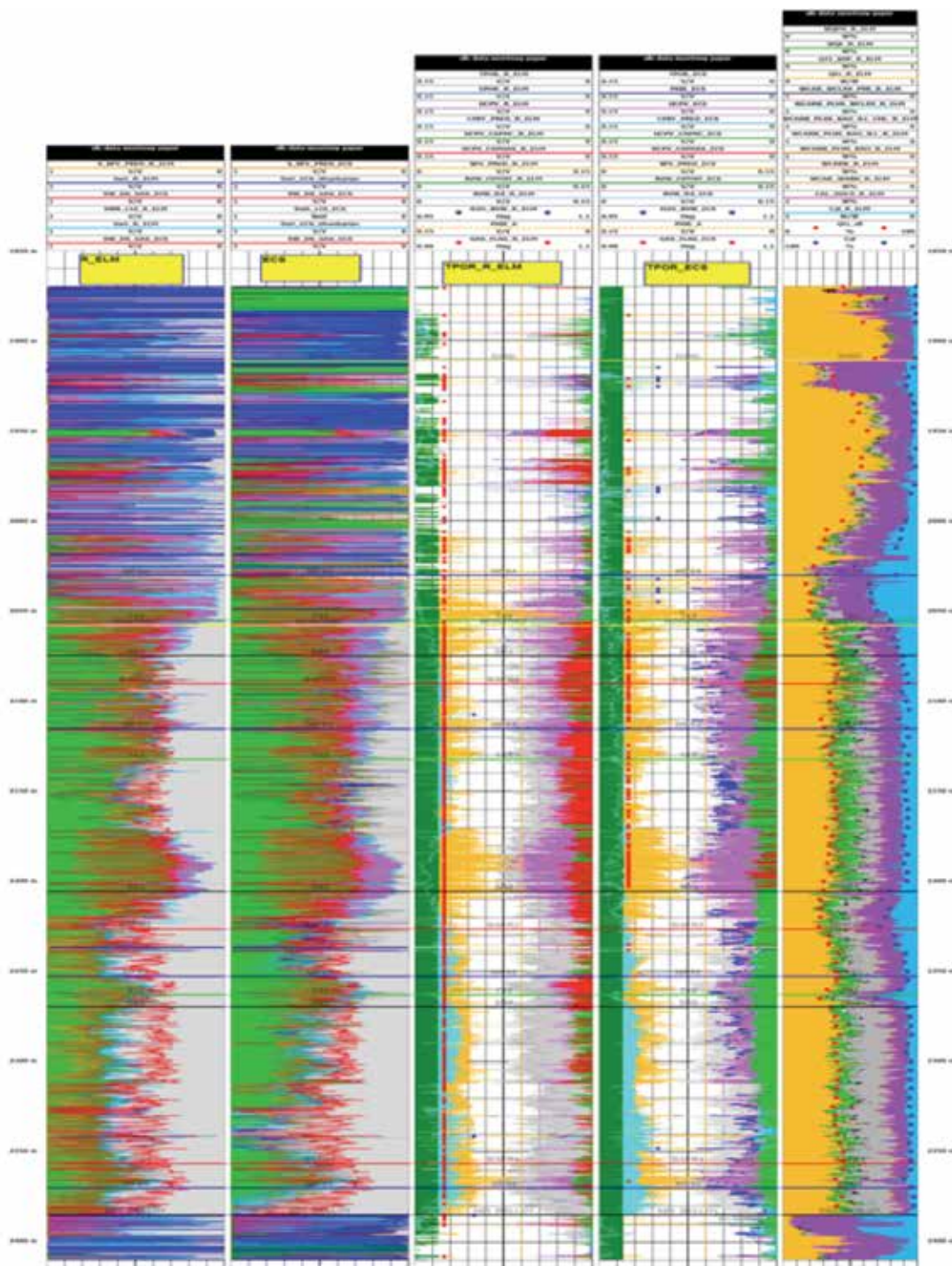


Figure F-9. Step 9: plot BVW (bulk volume of water, Sw^*TPOR); shade cyan from BVW left to BVW_CUTOFF to indicate water that would be free to produce in a non-shaly formation. However, having the NMR's BFV (orange) limits the producible water if the $BVW < BFV$, then no water is producible. When water is producible, the blue H2O_BVW flag turns on. Compare porosity to the Sw plot and ensure they tell the same story. In this case they do. Note there is some blue in the Sw track. This is not producible water but simply the Sw curve from the 0.0254 m/step data plotted on 1:180 scale.



Appendix G: Building the interpretation from Quick Look to Detailed

The figure consists of five vertically stacked spreadsheets, each representing a different stage of the well log interpretation process. The top spreadsheet is a 'quick look' pass, showing basic log data and initial calculations. The second spreadsheet introduces more complex calculations and labels for different geological layers. The third spreadsheet further refines the data, adding more detailed parameters and formulas. The fourth spreadsheet shows a more comprehensive set of calculations, including various correction factors and adjustments. The fifth spreadsheet is the most detailed, showing a wide range of calculated values and their relationships to the input data.

Figure G-1. Use the spreadsheet of Herron's equations (Ref. 4) to provide a quick look pass, using the core for elements. This can also be achieved by using a strip log description of the mineralogy and calculate elements for input to this Excel spreadsheet. Note, the use of spreadsheet is to give a user a sense of the equations. The Quick Look model is a subset of the PDHC program.

A	EG	EH	EI	EJ	EK	EL	EM	EN
1.05					ASSUME 80 %ILL, 20%CHLOR		RECORDED	
0.83							FOR	ESTIM FROM HURA
BELOW & CHECK TEMP FOR FEET	M2_Ds2	M7_Ds3				Model NPH	REFERENCE	8.1175
m	M2_Sh8	M12_Sh9		Fst_THPH	Mixr_THPH	M_NPH	NPH	TOC
1855.1652	0.9996	1		0.9000	0.0349		-0.9008	0.1075
1855.3176	0.9996	1		0.9000	0.0353		-0.9008	0.1075
1855.47	0.9996	1		0.9000	0.0354		-0.9008	0.1075
4456.5	1	1.0001		0.9000	-0.0003	0.0051	0.3486	0
4457	1	1		0.9000	0.0002	0.0084	0.3288	0
4457.5	1.0001	1.0001		0.9000	0.0002	0.0290	0.3424	0
4458	1	1		0.9000	0.0000	0.0430	0.3842	0
4458.5	0.9995	1		0.9000	-0.0005	0.0445	0.3853	0

Figure G-2. Result of first pass is shown next. Note there were no modifications made to the input data on this first pass. We simply want to see what it looks like before we modify. The notes on this plot (below) point out the modifications that are needed.

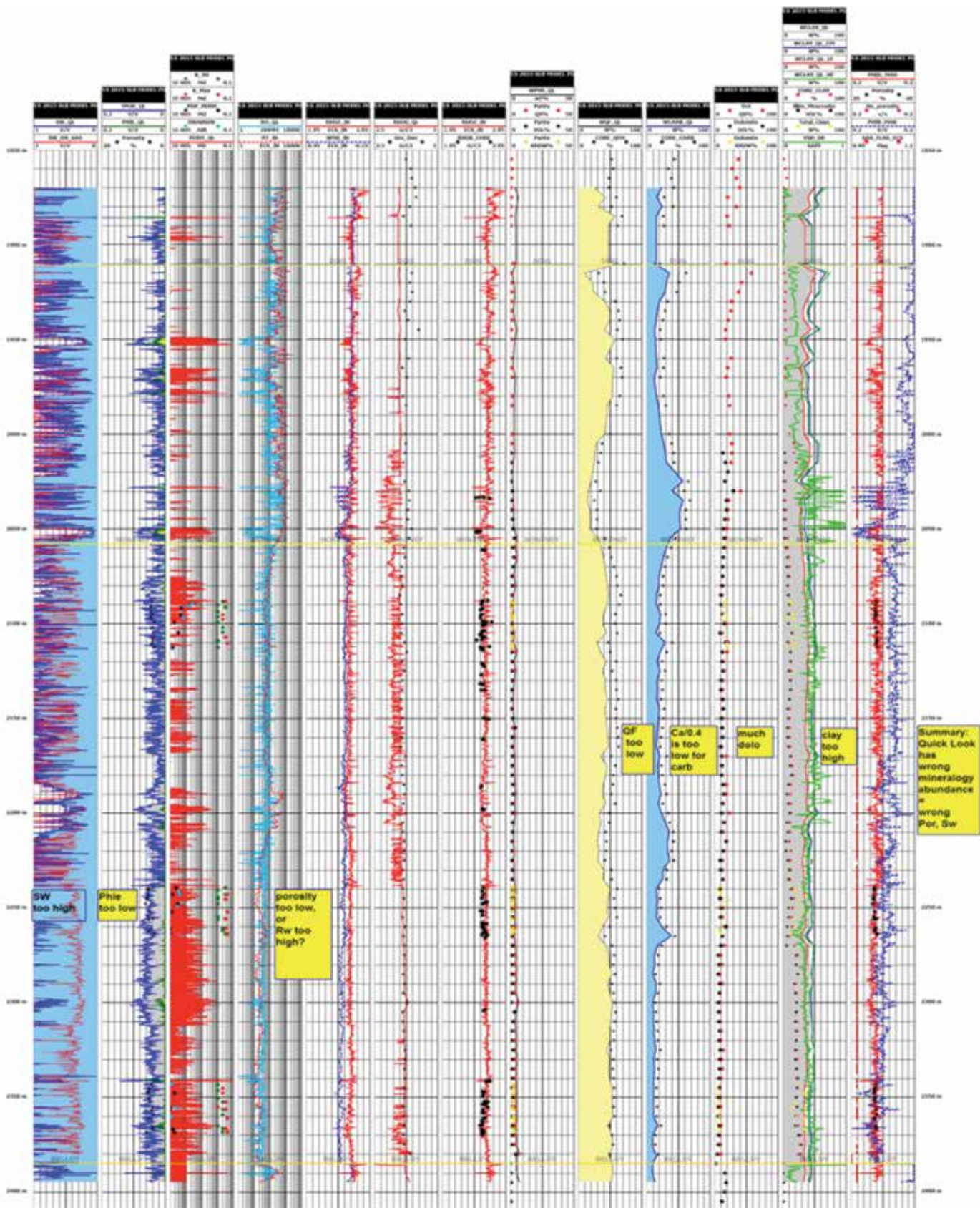


Figure G-2. Result of first pass is shown above. Comparison of core/cuttings mineralogy to Pass 1 mineralogy shows shortcomings of the Pass 1.



A	EG	EH	EI	EJ	EK	EL	EM	EN	EO	EP
1.05					ASSUME 80 %ILL, 20%CHLOR		RECORDED			
0.83							FOR	ESTIM FROM HURA	mult	multiply
BELOW & CHECK TEMP FOR FEET	M2_Ds2	M7_Ds3				Model NPPI	REFERENCE	0.1275	wclay_min	point 4 on
m	M2_Sh8	M12_Sh9		Est. TSPH	Shrs. TSPH	M. NPPI	NPPI	TOC		Ca/0.4
1855.1652	0.9996	1		0.8000	0.0349	0.0349	-0.0000	0.1075	0.5	0.8
1855.3176	0.9996	1		0.8000	0.0353	0.0353	-0.0000	0.1075	0.5	0.8
1855.47	0.9996	1		0.8000	0.0354	0.0354	-0.0000	0.1075	0.5	0.8
4456.5	1	1.0001		0.8000	-0.0003	0.0051	0.3498	0	0.5	0.8
4457	1	1		0.8000	0.0002	0.0084	0.3268	0	0.5	0.8
4457.5	1.0001	1.0001		0.8000	0.0002	0.0290	0.3424	0	0.5	0.8
4458	1	1		0.8000	0.0000	0.0430	0.2642	0	0.5	0.8
4458.5	0.9995	1		0.8000	-0.0005	0.0445	0.2823	0	0.5	0.8

Figure G-3. Modify the carbonate and clay on the spreadsheet by adding two columns at the end.

The carbonate was calculated as Ca / 0.4. But we saw from the Plot 1 that carbonate was too low. The reason it was too low is the dolomite portion is Ca / 0.22. So we estimate the combination of calcite and dolomite at Ca / 0.32 which is from Ca / 0.4 * 'mult2' or Ca / (0.4 * 0.8). We could also accomplish the same thing by 'Mult3' * (Ca / 0.4). The clay was too high compared to core so we multiply the clay by 0.5. The result is shown on the following page.

Worldwide Petroleum Consultants

Sproule: More than just a Reserves Evaluator

Sproule is a premier petroleum consulting and advisory firm that assists companies with the evaluation of oil and gas reserves and resources, M&A related due diligence and reservoir studies. But our expertise doesn't stop there. Sproule also prides itself on its team of qualified and experienced geoscientists and simulation engineers who offer Reservoir Characterization services such as:



Resource Assessments
Reserve Certification
Expert Witness

Reservoir Studies
Advisory Services
Academy

Learn more at www.sproule.com
Or email us at info@sproule.com

Geology

- Resource Estimation through a fully integrated probabilistic methodology
- Dedicated experts on prospective resource estimation processes

Geophysics

- Subsurface imaging
- Seismic 2D-3D-well mistie calibration and grid balancing
- Advanced 2D and 3D seismic data interpretation
- Complex structural mapping
- Seismic trace, horizon and interval-based attribute analysis
- 3D voxel-rendering and visualization

Petrophysics

- Single Well to Field-Wide studies
- Evaluation of effective porosity and water saturation
- Interpretation and integration of routine and special core analysis
- Analysis of wireline pressure measurements
- Capillary pressure data and saturation height functions, reservoir rock typing and flow unit characterization

Geomodelling

- Subsurface Geology
- Use of Geostatistics to measure and quantify data uncertainty for optimal drilling strategies
- Basin Modelling

Reservoir Simulation

- Reservoir characterization
- Black oil
- Compositional thermal complex gathering systems
- Surface networks
- Field development planning and migration issues

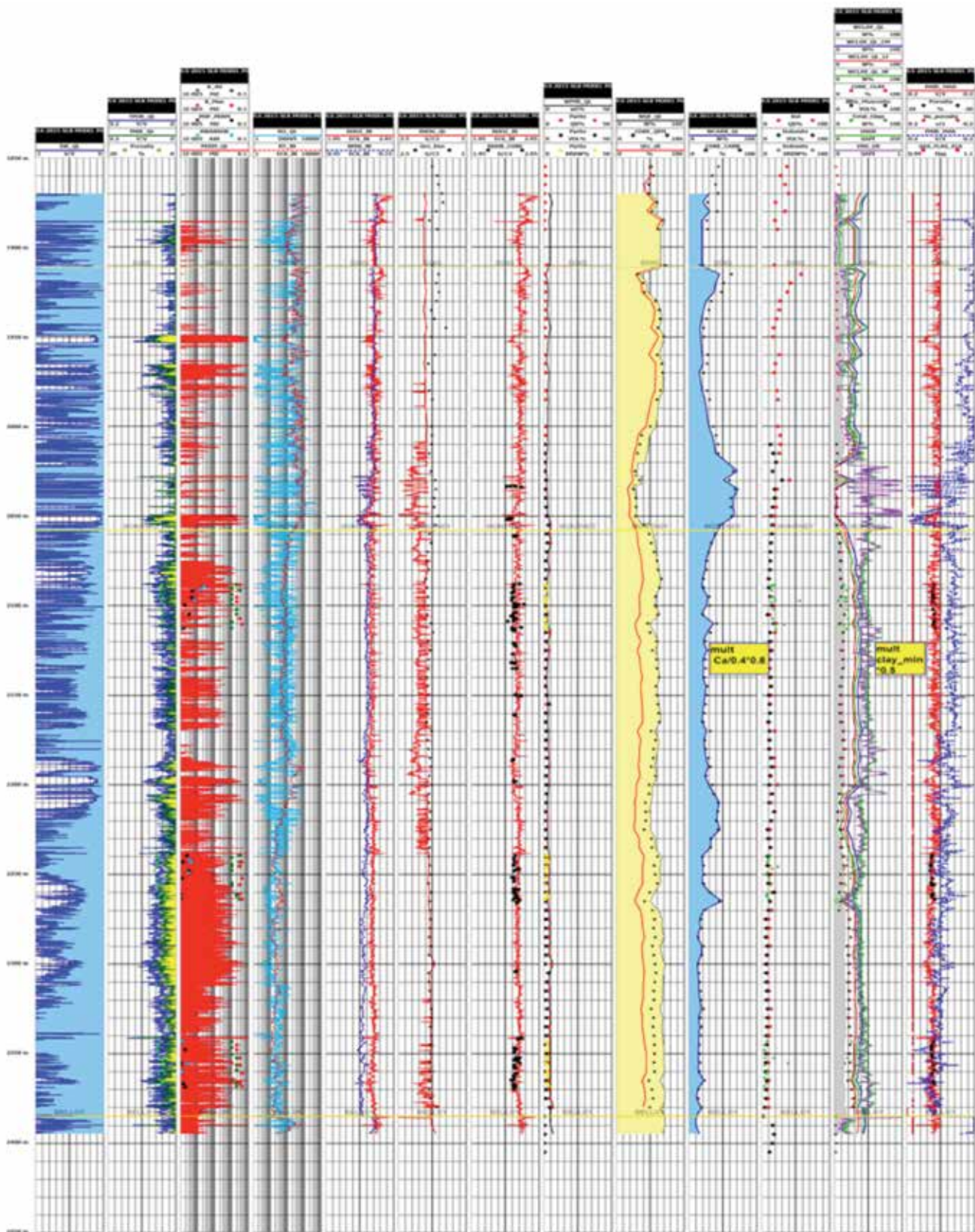


Figure G-4. Result of modification. We have the mineralogy pretty close. We now add another column for the SW_DS_GAS in Track 1, Figure G-5, next.

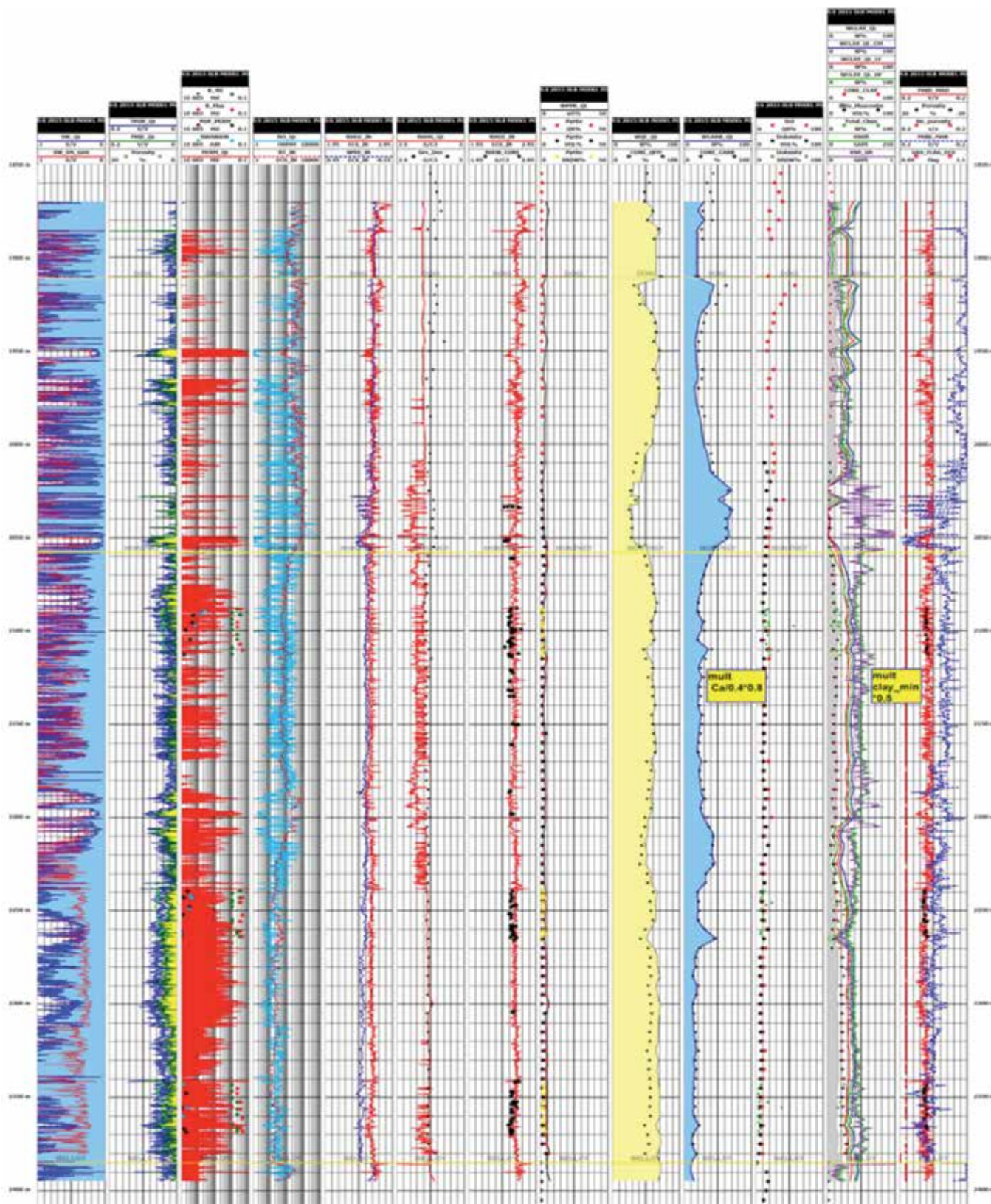


Figure G-5. Result of modification by adding Sw_DS_Gas. Now we have more questions: is the yellow effective porosity going to produce water? Looking at the Sw plot, it appears it will. However we have clay, so what is the effect of the clay? Plot Swb.

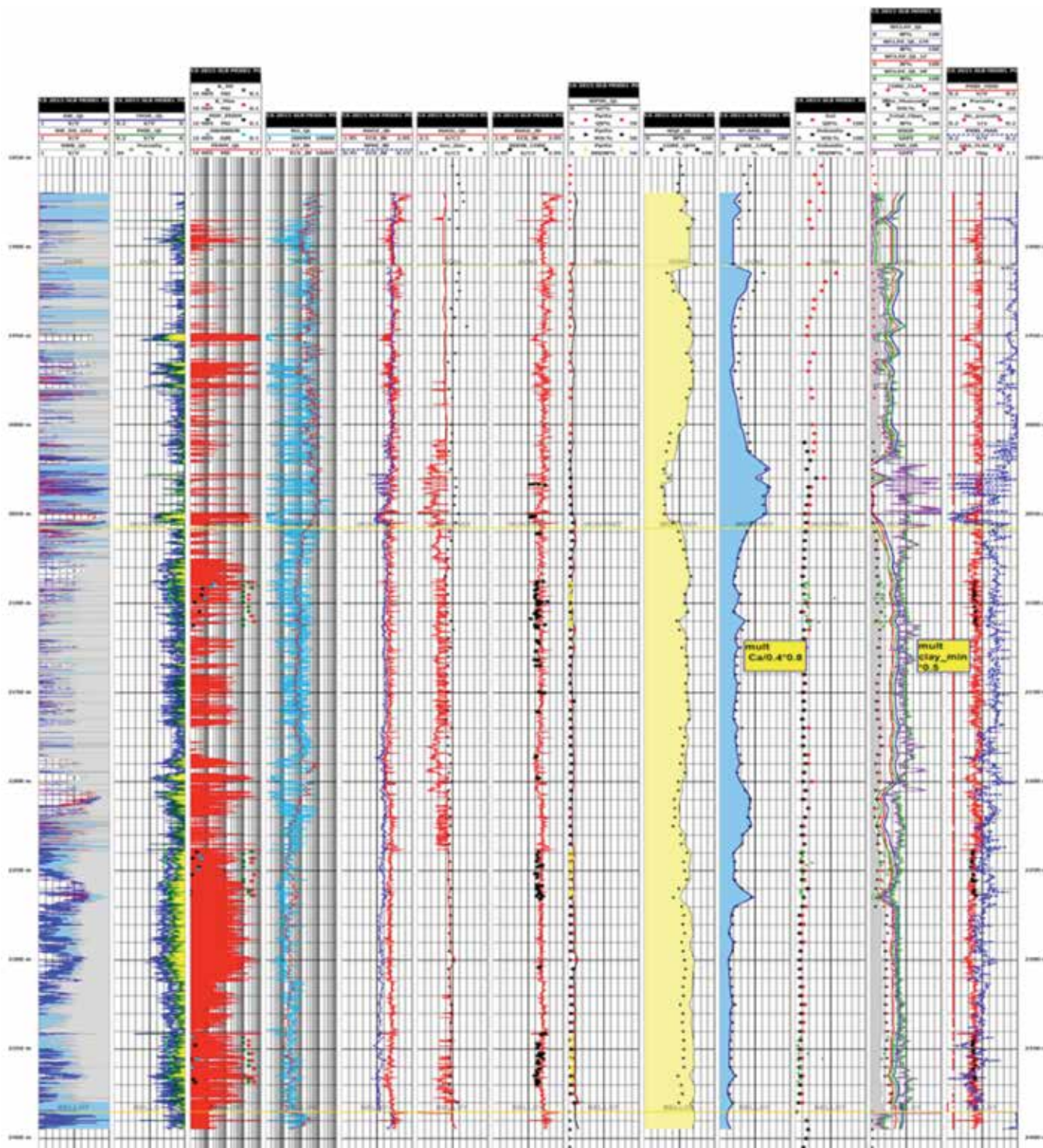


Figure G-6. Result of modification by adding Swb. A reminder on how Swb was calculated: all the clay was assumed to be illite. Looking at the core mineralogy this seems to be reasonable. Swb involves CEC, Q_v , mol weight and a formula relating them, $(0.22 + (0.084 / (\text{Mol wt}^{0.5})))$. But the Swb appears to be too high. So, now we have to do something better than this quick look method.

With the addition of the CMR and LithoScanner we can refine the porosity and Sw. So we come full circle to the detailed interpretation shown next.

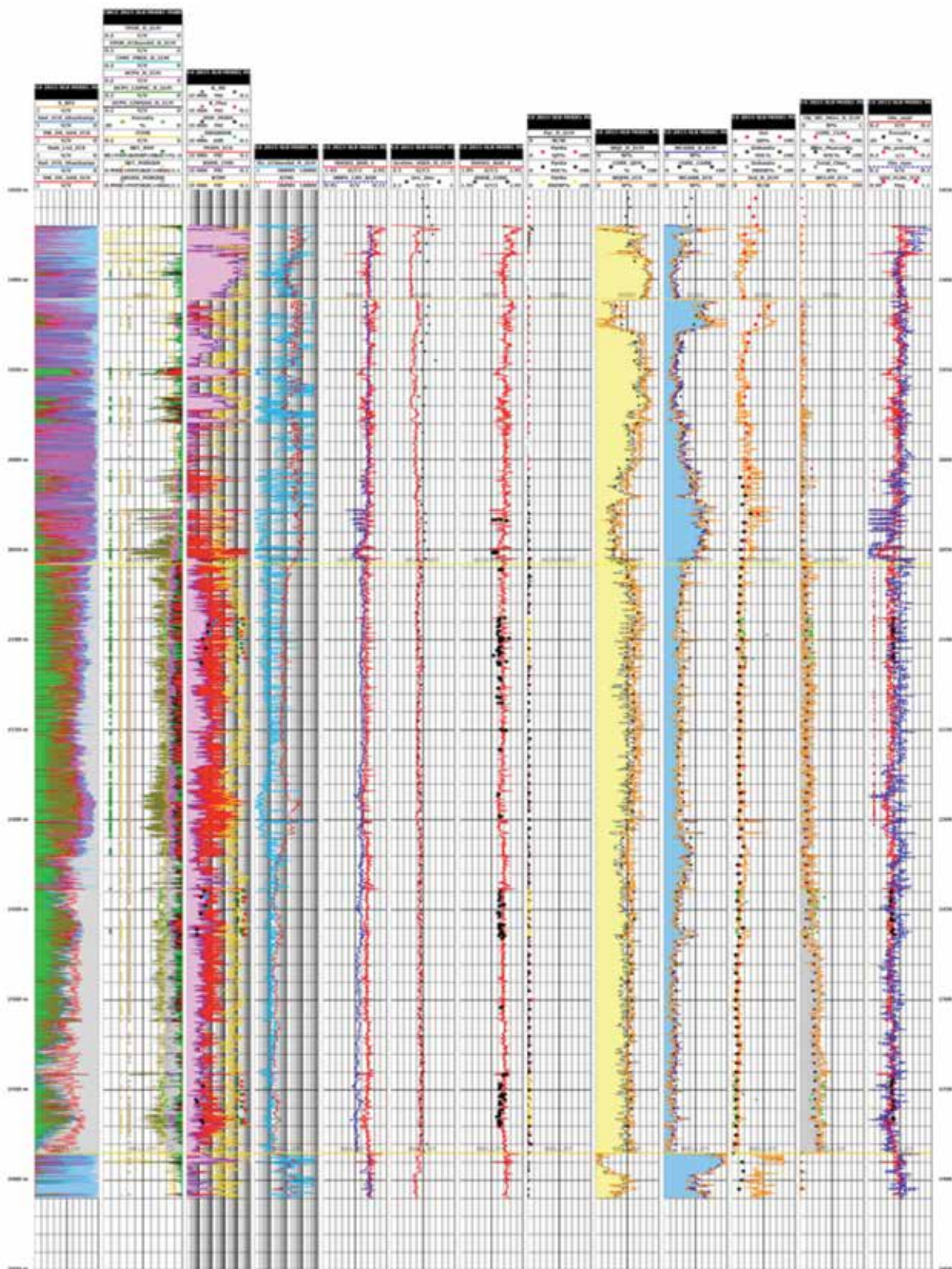


Figure G7. Result of detailed interpretation, adding the NMR and Logs of elements plus applying some limits.



Bottom Line: Using core/cuttings mineralogy, elemental capture spectroscopy and nuclear magnetic resonance results in a valid interpretation where the logs and the mineral analysis honour each other. This illustrates the method we call 'Petrophysics Designed to Honour Core'.

Appendix H: Summary of Techniques used:

1. SP to convert a known R_w at one depth to a variable R_w for all depths.
2. A crustal relationship noted by Dr. Susan Herron is that $U = 0.3 * Th$. This gives a quality check on the Uranium and Thorium curves. When there is excess Uranium, $U - 0.3 * Th = \text{Excess Uranium}$, then bitumen and/or kerogen may be the reason. Apparently the uranium was dissolved in the water when the oil/water was migrating. When migration stopped, the water was squeezed out and the uranium was left with the bitumen.
3. m^* and m_zero are derived from the Herron relationships.
4. $CEC = \text{Sum}(W_i * CEC_i)$
5. Surface area, $SO = \text{sum}(W_i * SO_i)$
6. Matrix density is derived from the Herron relationships. It is subsequently modified a small amount using the TOC in the output called RHOG_ECS. Matrix density modifies a large amount using TOC in the output called RHOG_KER_ECS. The term 'ECS' is used to denote the equations were derived for the ECS interpretation, primarily by the Herron's.
7. Bad hole is checked by comparing porosity-Wylie-sonic using 47.5 usec/f to porosity from the density log using 2.71 g/c3.
8. Predictions of curves from one well to another are accomplished using cluster in the GAMLS code.
9. Pay flags are derived using the pay criteria in Appendix B.
10. Swirr involves porosity and grain density.
11. Sw_crit involves free fluid porosity.
12. $Sw_DS_Gas * \text{porosity} * \text{multiplier}$ is used to provide a BVW cutoff.
13. Rt_Pay and $RT_PayMultiplier$ are derived from Sw_DS_Gas .
14. Saturation of the bound fluid volume is used as a limit to determine what part of the water saturation is free and what is not free. $S_BFV = BFV / \text{Total porosity}$.

Most of the equations were not invented by the author but were gathered from other sources and put together into a program called Petrophysics Designed to Honour Core (PDHC) written in Java by my son, Jamie Everett from my humongous Excel-generated spreadsheets. References cited are the source of the equations' authors. If we have omitted a reference please advise. We are attempting to use, not plagiarize, the ideas of others in the spirit that they were made available through their publications. Equations in excel format or the 'HerronPapers.zip' may be requested via Robert V Everett Petrophysics web site by email (at no charge) in the interest of promoting the use of spectroscopy for interpretation. All equations are explained, used, and taught in the annual 'Petrophysics using Spectroscopy' course presented in conjunction with the GeoConvention for CSPG/CSEG/CWLS. Spectroscopy-based interpretation methods were designed in the 1980s to replace Vshale methods to improve log-derived estimates of porosity, water saturation and permeability. However, the methods are not yet generally available in commercial software packages. The programs GAMLS and PDHC do have the methods and are available. We do not sell PDHC (there is a patent by Drs. Susan & Michael Herron with Schlumberger of Canada on their program) but do charge a maintenance fee to keep your software copy updated. We are constantly updating and making it easier to use. The author routinely uses the spectroscopy methods for all log interpretation. Measured elements are preferable (LithoScanner™, ECSTM, FLEXTM, GEMTM). X-Ray Fluorescence (XRF), elements derived from QemScan™ and/or log-predicted elements are a second choice. Predictions via clustering should be made from wells with measured elements in the same depositional environment. Hence, at least one set of measured elements per field is the goal. The prediction method uses a mean and standard deviation, amongst other attributes, so there is necessarily some averaging/smoothing involved. For high resolution, it is infinitely better to use measured values.



Sponsors



Canbriam



Exshaw Formation overlying the Palliser and overlain by the Banff formations, Goat Creek, Alberta.



Cardium Formation at Horseshoe Dam, Bow River, Alberta.

Photos courtesy of Per Kent Pedersen, Associate Professor, Department of Geoscience, University of Calgary

A high resolution .pdf of the latest InSite is posted on the CWLS website at www.cwls.org. For this and other information about the CWLS visit the website on a regular basis.

For information on advertizing in the InSite, please contact:

Doug Kozak
doug.kozak@halliburton.com (403) 998-1966

Manuel Aboud
maboud@slb.com (403) 990-0850

Discounts on business card advertisement for members.

Technical Experts. Global Expertise. Local Solutions



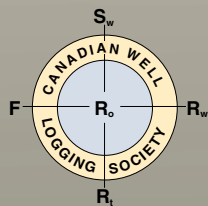
- **Well-site Services**
- **Helical CT Scanning**
- **Routine Rock Properties**
- **Special Core Analyses**
- **Geological Services**
- **Reservoir Fluid Analyses**

Contact Us:

403-250-4000

PSCanadaSales@corelab.com

www.corelab.com



CANADIAN WELL LOGGING SOCIETY

Scotia Centre 2200, 700 – 2nd Street S.W., Calgary, Alberta T2P 2W1

Telephone: (403) 269-9366 Fax: (403) 269-2787

www.cwls.org